The role of silicon in investment casting. A study of the reactivity of various metals with the investment

1. Summary

It is well known that in the investment casting of gold alloys silicon enables to obtain better mould filling and deoxidised castings.

Up to now it has been believed that silicon as alloying addition or through the formation of SiO2 could be sufficient to explain the deoxidised appearance of the cast tree and the good filling of the mould.

Preliminary analyses suggested that silicon dissolved in the liquid phase could form a compound with high surface tension that can form a thin film on the outer surface of the molten metal. This film restrains the evaporation of zinc and other metals, whose evaporation temperature is lower than the temperature of the molten alloy. In the case of investment casting, this film minimizes the contact between the components of the alloy and the mould wall, even if a reaction with calcium sulphate and/or its decomposition products (oxygen and sulphur dioxide) cannot be excluded.

It is presumed that the reaction between the components of the alloy and the decomposition products of calcium sulphate will be minimized and that the thin film will facilitate the flow of the metal on the surface of the mould cavity, making mould filling easier.

2. Introduction

This work intends to clarify the effect of silicon in investment casting of carat gold alloys. 14 ct yellow gold alloys have been considered.

According to our experience, the deoxidising effect of silicon is enhanced by the presence of zinc. For this reason also the interaction between Zn and Si has been investigated.

Various studies have already shown that even very small additions of silicon can guarantee a clean and bright surface on the castings and an improved filling of the mould. The highest acceptable Si concentration in the gold alloy has already been specified in many articles. This Si concentration depends on the fact that excess silicon can cause problems, like alloy embrittlement and grain growth. As far as grain growth is concerned, it has been observed that Si not only causes grain growth, but also inhibits the effect of most grain refiners.

In conclusion, as reported in the scientific papers, the beneficial effects of silicon addition to yellow gold alloys are already appreciable with very low silicon concentration. Therefore a large part of the studies on this subject has principally addressed the highest Si concentration that can be tolerated before the adverse effects become disturbing.

In particular, for 14 ct yellow gold, the highest acceptable Si concentration has been set to 2500 p.p.m. (parts per million), because above this level the material becomes fully embrittled, even if it should be advisable not to exceed 900 p.p.m., to preserve the good characteristics of the alloys.

However there are not studies to clarify the actual mechanism enabling Si to give protection against oxidation. Presently Si is simply added to the gold alloys to reduce the effect of oxygen and increase fluidity.

Silicon shows some solid state solubility in copper, but it is insoluble in solid gold and silver. Silicon reacts with oxygen much more readily than Zn and Cu. It is assumed that Si protects the molten metal by combining with all available oxygen, and transforming into silica (SiO2), that forms a thin, invisible layer on the surface of the castings.

Up to now probably the role of zinc has not been completely clarified. The ability of zinc to improve wettability of the molten metal and mould filling ability is well known. Zinc shows also deoxidising activity, mainly in the case of casting in air. A maximum Zn concentration of 2% wt is recommended, because at higher concentration it tends to form intermetallic phases with all the components of the alloy.

The ambitious aim of this study is to clarify the mechanism of the action of zinc and the effect of the interaction between Zn and Si in the gold alloys.

When considering the role of Si in investment casting, also the behaviour of the investment should be taken into account, when it comes into contact with the hot metal. The various studies carried out on this subject evidenced principally a decomposition of calcium sulphate, that takes place at 1200°C, according to the reaction $CaSO4 \rightarrow CaO + SO2 + ½\ O2$. This reaction is catalysed by silica, that lowers the decomposition temperature of CaSO4.

3. Preparation of the samples

16 flasks with 16 different alloy compositions have been cast. The concentration of gold (585 ‰) and silver (40 ‰) has been kept constant. In the first set of 8 flasks the following additions of zinc have been made 0, 10, 20, 30, 40, 60, 80 100 ‰, balance copper. In the second set of 8 flasks, the composition is the same as in the first set, with the difference that 500 p.p.m. of silicon have been added in each alloy, at the expense of copper. The composition of the 16 alloys is shown in Table 1.

For the experiments the Ultra-vest investment powder of Ransom & Randolph has been used. Usually investment powders are composed of a mixture of calcium sulphate hemihydrate ($2CaSO4\ .\ H2O$) that acts as a binder (25 – 30%) and crystalline silica (70 – 75%), in the form of quartz and α–cristobalite, that is the actual refractory.

The concentration of controlling additions is stated by the producer as lower than 5%wt.

Table 1 – Composition of the alloys (wt‰)

Alloy	Au	Ag	Cu	Zn	Si
543	585	40	375	0	0
544	585	40	365	10	0
545	585	40	355	20	0
546	585	40	345	30	0
547	585	40	335	40	0
548	585	40	315	60	0
549	585	40	295	80	0
550	585	40	275	100	0
628	585	40	374,5	0	0,5
629	585	40	364,5	10	0,5
630	585	40	354,5	20	0,5
631	585	40	344,5	30	0,5
632	585	40	334,5	40	0,5
633	585	40	314,5	60	0,5
634	585	40	294,5	80	0,5
635	585	40	279,5	100	0,5

Before use, the alloys have been melted in an induction furnace and cast into ingot, with a casting temperature of 1020°C. The ingots have been rolled and cut into pieces, to improve composition homogeneity. The subsequent casting operation has been carried out in a casting machine with controlled atmosphere. A different casting temperature has been used for each alloy: it was 100°C higher than the liquidus temperature, that has been determined with DTA (differential thermal analysis). All flasks have been kept 10 min. at room temperature after casting, then have been quenched into water.

The shape of the castings has been selected on the basis of the planned research. Therefore 3 spheres of different size have been cast. The spherical shape has been preferred, to facilitate the occurrence of a reaction between the metal and the investment. This is because, for the same volume, the sphere has a smaller surface than any other shape and consequently a lower rate of heat exchange.

Three different sizes of the spheres should enable to evaluate the effect of thermal mass in the process, to see if a change of the amount of released heat could affect surface quality (due to reactions between the metal and the investment).

The spheres we used had the following diameters: 15.4, 12.6 and 10.2 mm respectively. The feed sprues had round cross section and diameter of 5, 4 and 3 mm respectively, Figure 1.

Also the pressure applied after casting plays an important role, because a higher pressure favours the reaction between metal and investment. A constant overpressure of 2 kg/cm2 has been used in all cases. In our opinion, this overpressure represents a good compromise between surface quality of the castings and mould filling.

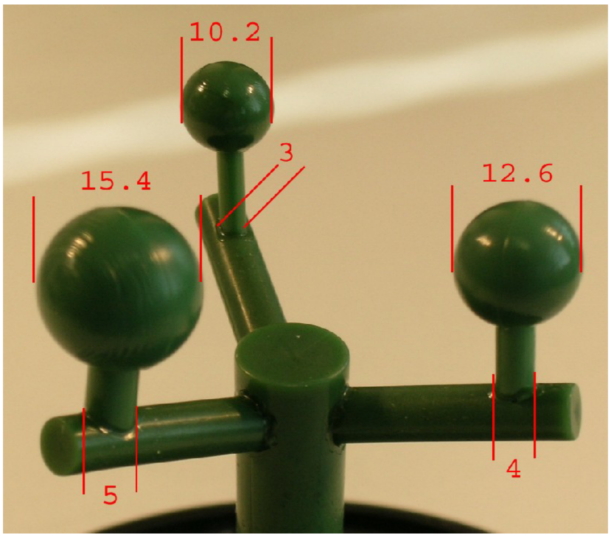

Figure 1 – Size of the cast samples

4. Experimental results

Firstly the silicon free samples have been investigated (samples 543 to 550).

The investment has been removed from the cast trees with a high pressure water jet. Then the cast spheres have been separated from the tree.

Pictures of the surface of the spheres have been taken with a zoom stereoscopic microscope with 10x magnification, in order to evaluate surface quality. No significant difference has been observed among the surface quality of the spheres with different size and the same composition: therefore only the pictures of the biggest spheres are reported here.

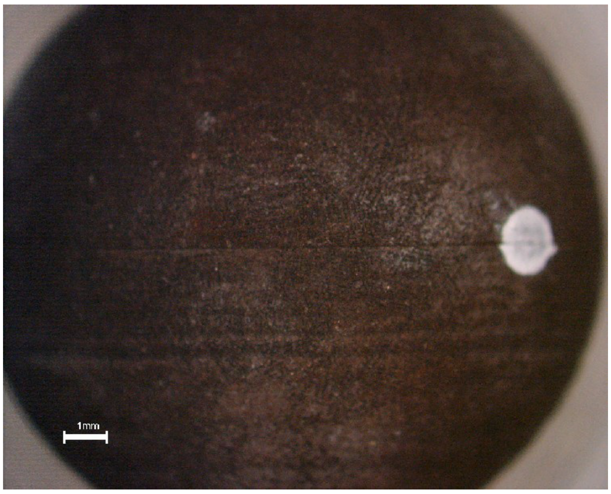

Sample 543

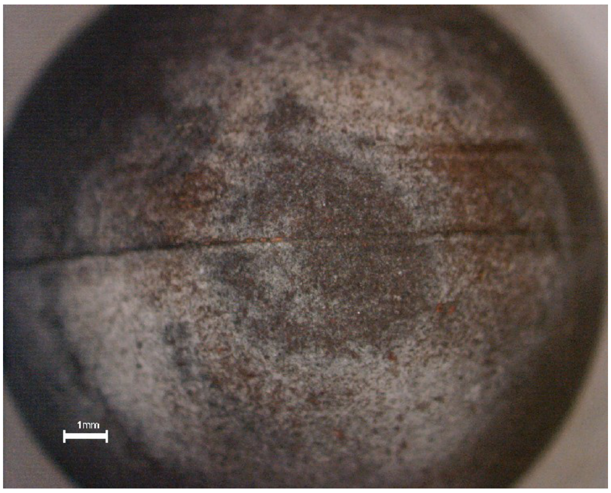

Sample 546

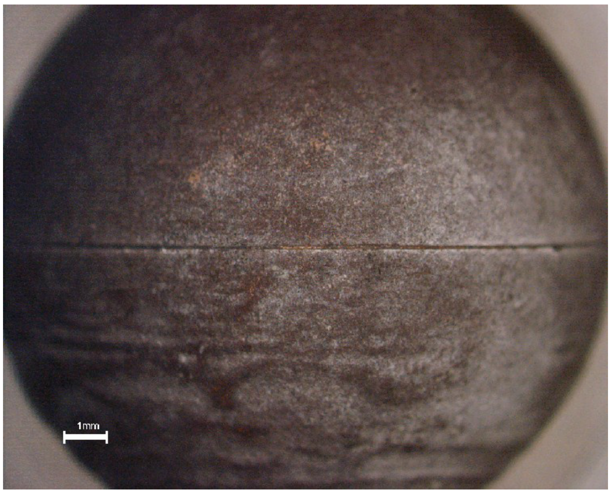

Sample 544

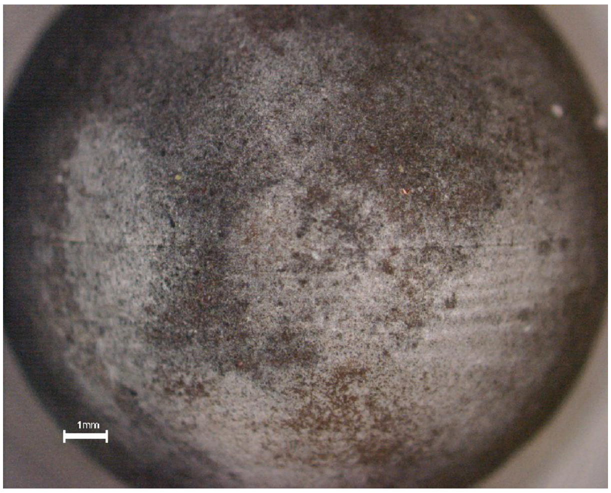

Sample 547

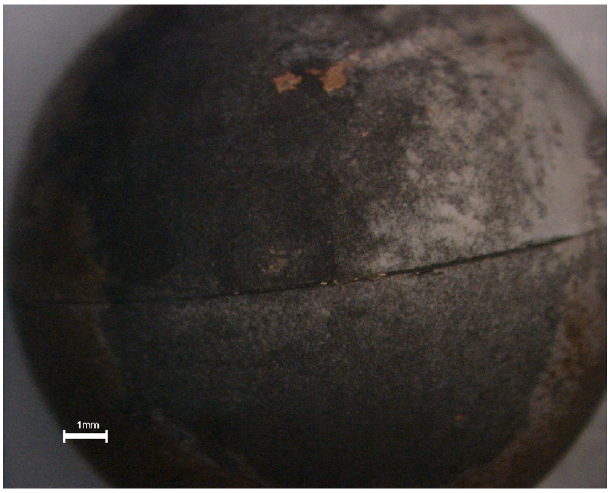

Sample 545

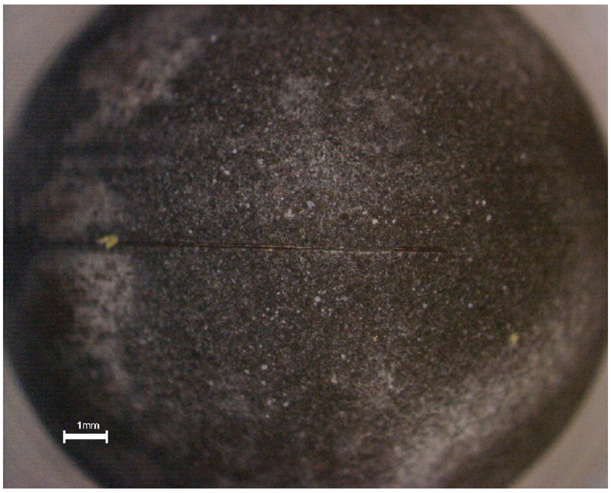

Sample 548

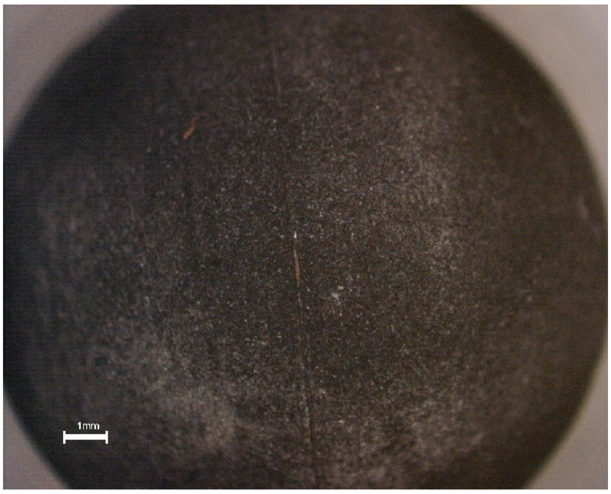

Sample 549

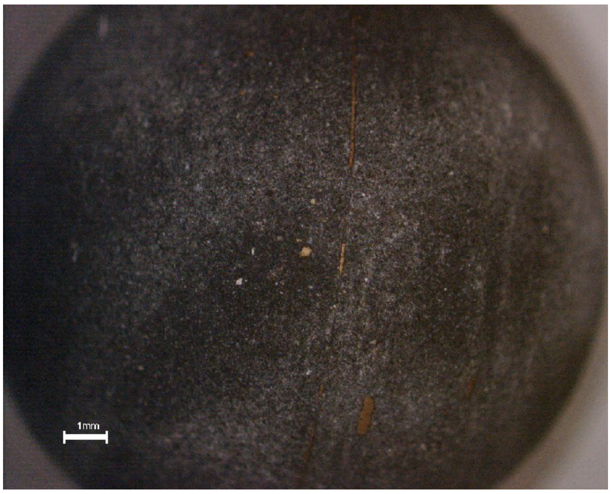

Sample 550

Figure 2 – Surface of the spheres – As cast - Samples 543 to 550 (Si free alloys)

The appearance of the surface of the as cast spheres suggests that an intense reaction occurred between metal and investment. Then we have analysed the surface of the spheres with EDS (Energy Dispersion Spectroscopy of X rays) under a XL30 Philips scanning electron microscope (SEM). At the beginning of the work we had planned to analyse 3 points on each sphere, i.e. the apex (point A) and two more points on a great circle (points B and C), Figure 3.

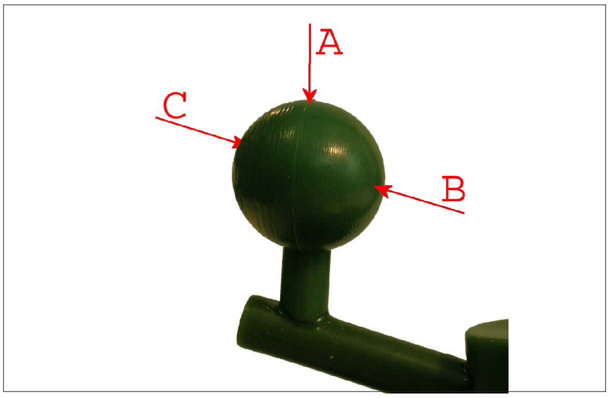

Figure 3 – Analysed zones on the sphere

The analyses carried out in the points A, B and C gave similar results, therefore it has been decided to go on by making analyses only in the point A.
The concentration of various elements in the surface of the castings, determined with EDS microanalysis, is shown in Table 2 for the first set of alloys.
The samples are denoted with the code number (Table 1) preceded by a letter: G for the bigger sphere, M for the medium sphere and P for the smaller one. We know that the instrumental precision is not so deap (especially for Si,C, O...) but we have automatical acquiring of datas and we report values as they were.

Table 2 – As cast silicon free castings (samples 543 to 550). Surface composition

sample	Elements [wt%]									
	C	O	Si	S	Ag	Ca	Cu	Zn	Au	Others(Mg, K, Al, Ti)
G543	6.86	19.55	13.01	4.56	0.65	6.07	44.40	0	4.16	0.74
M543	13.01	16.32	11.89	5.37	0.60	7.87	39.88	0	4.30	0.76
P543	6.51	19.58	12.83	5.31	0	6.82	41.8	0	5.84	1.30
G544	3.86	24.12	16.45	8.99	0	12.34	24.48	6.24	3.10	0.42
M544	4.77	16.61	7.75	5.82	1.40	7.58	34.92	6.17	13.26	1.72
P544	2.81	23.75	16.71	6.57	0	10.29	25.56	11.91	0	0
G545	5.19	28.66	19.77	6.77	0	9.71	18.52	10.89	0	0.49
M545	9.02	21.00	10.23	6.60	0.86	8.04	23.20	10.28	9.92	0.84
P545	5.92	18.37	9.64	8.07	0.69	9.15	18.55	18.20	10.58	0.83
G546	6.00	25.31	26.27	3.56	0	6.50	18.91	13.44	0	0
M546	4.99	13.84	4.02	6.36	1.88	4.61	22.77	12.86	28.66	0
P546	6.73	24.72	25.48	3.66	0	5.88	21.78	11.76	0	0
G547	3.20	25.97	23.73	6.61	0	10.47	9.81	19.34	0	0.86
M547	4.59	22.98	23.26	5.27	0	6.84	16.13	19.81	0.88	0.23
P547	9.44	27.45	23.49	5.70	0	7.27	10.52	15.64	0.49	0
G548	6.30	19.36	24.03	0	0	6.07	19.92	24.32	0	0
M548	14.36	24.36	20.50	4.49	0	4.82	12.61	18.63	0.24	0
P548	6.79	20.47	13.67	8.19	0	10.03	10.30	23.87	6.86	0
G549	1.57	20.80	24.12	4.93	0	5.00	14.94	28.33	0	0.30
M549	4.02	26.18	26.76	4.57	0	5.80	9.95	22.63	0	0
P549	15.92	22.38	12.90	7.47	0	7.94	8.40	21.37	3.33	0.30
G550	13.96	23.80	19.60	4.89	0	6.20	10.31	21.02	0	0.23
M550	3.71	26.93	24.34	5.72	0	8.46	8.04	21.71	1.09	0
P550	8.61	22.98	18.19	6.82	0	6.92	6.67	27.79	1.35	0.67

*G = large sphere; M = medium sphere; P = small sphere

After analysing, the surface of the cast spheres has been pickled in a solution of hydrofluoric acid, followed by rinsing in an ultrasonic washing tank, to remove the reaction products.
Pictures of the surfaces have been taken with the stereoscopic microscope after pickling with hydrofluoric acid, Figure 4.

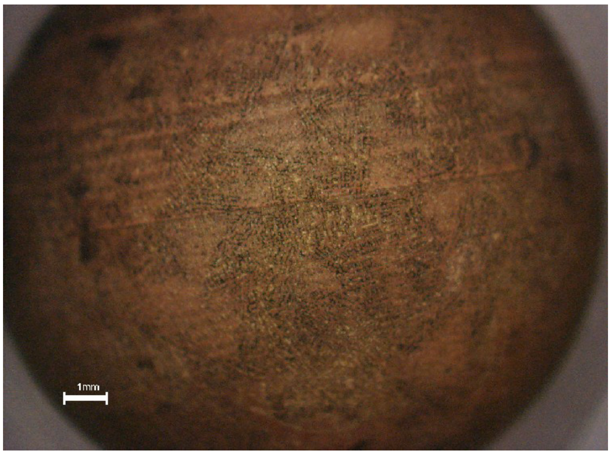

Sample 543

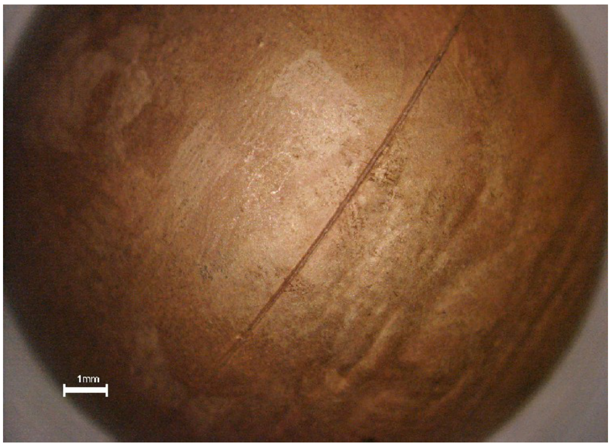

Sample 544

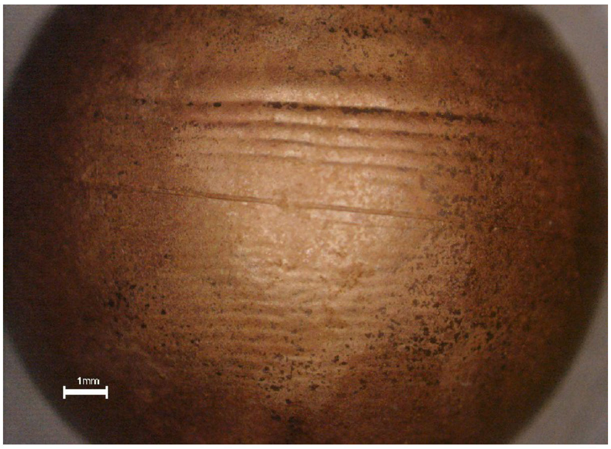

Sample 545

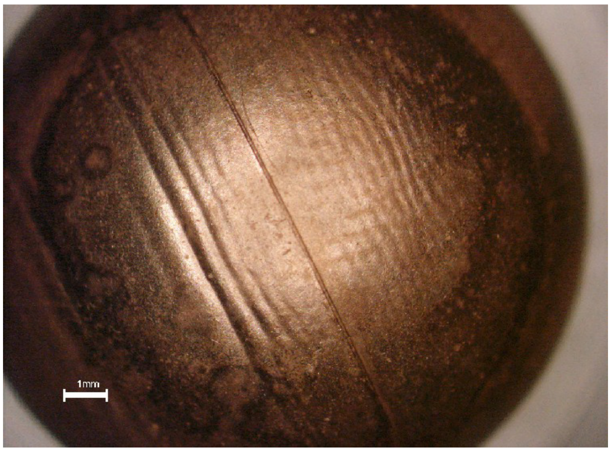

Sample 546

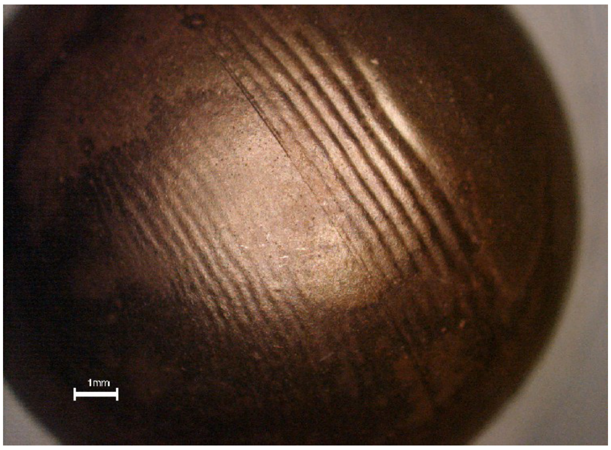

Sample 547

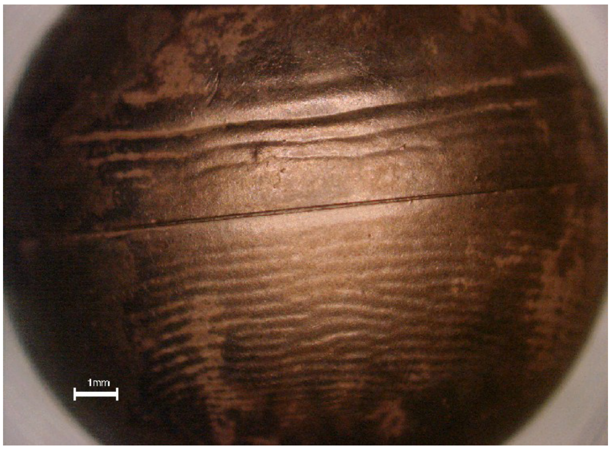

Sample 548

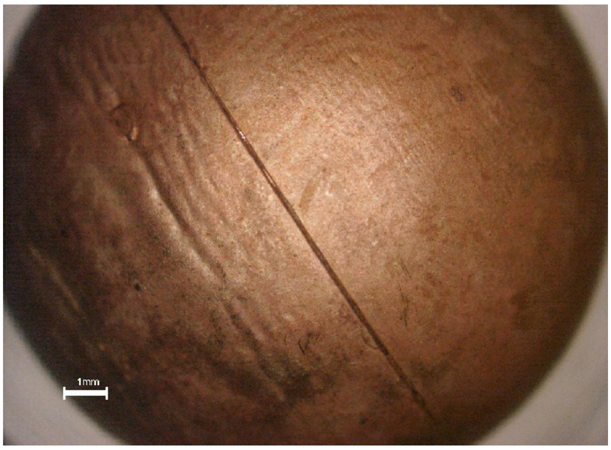

Sample 549

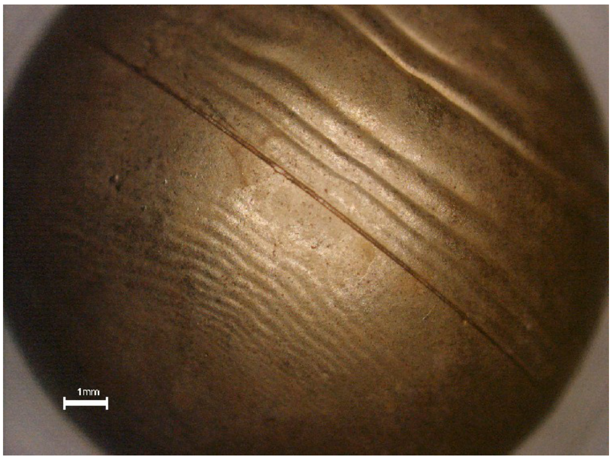

Sample 550

Figure 4 – Surface of the spheres after pickling with hydrofluoric acid Samples 543 to 550 (Si free alloys)

The results of the microanalysis carried out in the same points as before are shown in Table 3.

Table 3 – Composition of the surface of the samples 543 to 550 (Si free alloys) after pickling with hydrofluoric acid

sample	Elements [wt%]									
	C	O	Si	S	Ag	Ca	Cu	Zn	Au	Others(Mg, K, Al, Ti)
G543	0	6.19	0	0	8.59	0.68	17.43	0	67.11	0
M543	3.29	3.85	0	0	6.79	0.39	20.44	0	65.23	0
P543	3.92	4.29	0	0	7.78	0	16.13	0	67.88	0
G544	3.12	1.22	0	0	8.07	0	17.10	0	70.50	0
M544	2.20	1.05	0	0	10.26	0.25	14.83	0	71.41	0
P544	2.06	0.95	0	0	7.44	0	20.26	0.24	69.05	0
G545	3.32	1.53	0	0	8.27	0.07	18.67	0.50	67.64	0
M545	2.57	1.51	0	0	9.42	0.07	16.87	0.36	69.20	0
P545	3.73	1.66	0	0	5.23	0.04	27.72	0.29	61.32	0
G546	2.57	1.29	0	6.73	4.77	0	25.20	0.45	59.00	0
M546	0	1.79	0	4.91	4.42	0	30.22	2.16	56.49	0
P546	0	1.99	0	4.60	4.80	0	22.28	0.50	65.83	0
G547	0	1.92	0	6.15	3.47	0	29.77	1.61	57.07	0
M547	0	1.54	0	5.83	3.68	0	27.91	0.80	60.25	0
P547	0	1.70	0	5.52	3.57	0	29.30	1.04	58.88	0
G548	0	2.47	0	10.18	2.90	0	32.16	0.65	51.64	0
M548	0	2.71	0	8.63	2.99	0	31.63	0.99	53.04	0
P548	0	2.87	0	0	4.44	0	30.94	3.85	57.90	0
G549	0	1.58	0	7.08	2.77	0	26.86	5.76	55.95	0
M549	0	1.26	0	6.13	2.57	0	27.69	6.26	56.08	0
P549	0	2.47	0	0	3.39	0	28.06	6.09	60.00	0
G550	0	2.42	0	7.32	3.64	0	23.92	9.46	53.23	0
M550	0	1.89	0	0	3.62	0	25.50	9.01	59.98	0
P550	0	1.48	0	0	2.89	0	27.31	7.40	60.92	0

***G = large sphere; M = medium sphere; P = small sphere**

The same procedure has been followed for the examination of the silicon containing castings. Therefore pictures of the as cast surface of the spheres have been taken, Figure 5.

Sample 628

Sample 629

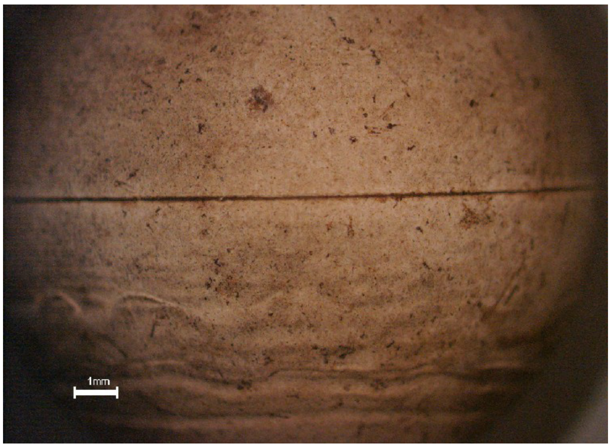

Sample 630

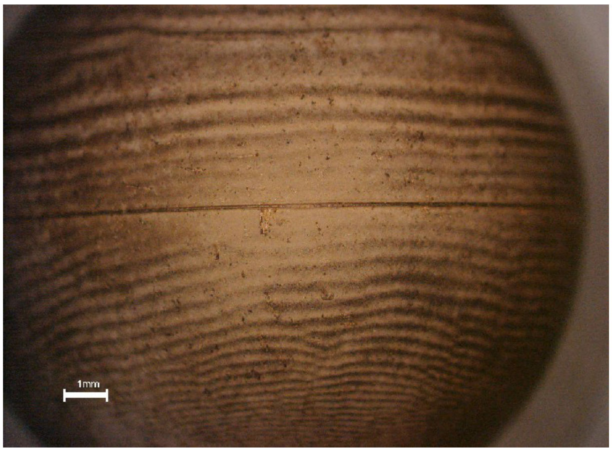

Sample 631

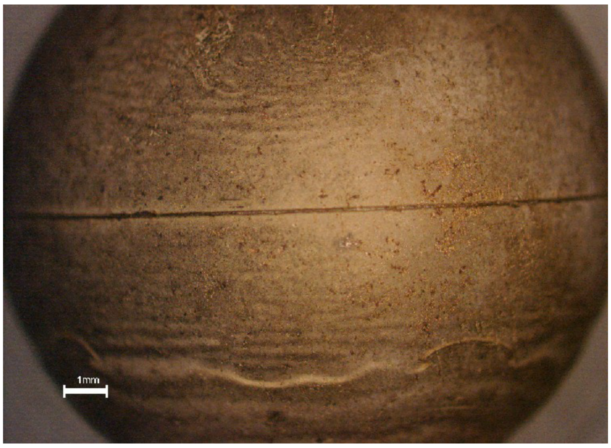

Sample 632

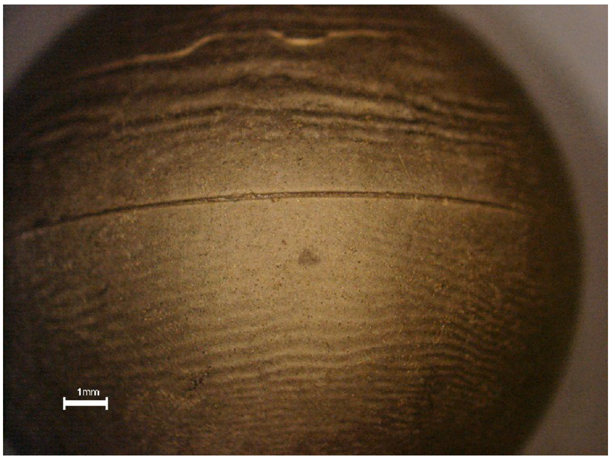

Sample 633

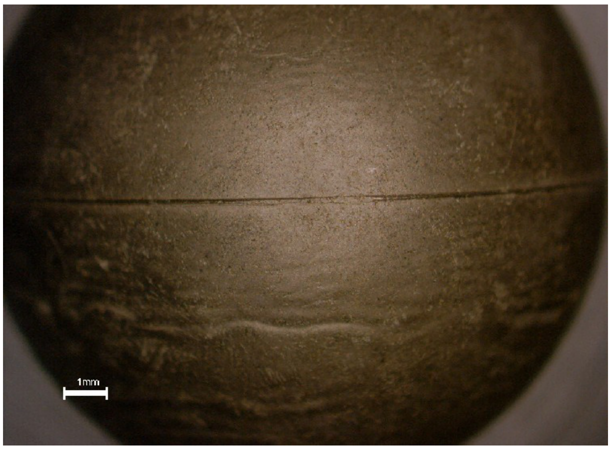

Sample 634

Sample 635

Figure 5 – Pictures of the surface of the silicon containing castings (samples 628 to 635) – As cast.

The observation suggests that in this case no interaction occurred between the metal and the investment. Subsequently the surfaces of the as cast spheres have been submitted to microanalysis. The results are shown in Table 4.

Table 4 – Silicon containing castings (Samples 628 to 635). Surface composition – As cast

sample	Elements [wt%]									
	C	O	Si	S	Ag	Ca	Cu	Zn	Au	Others(Mg, K, Al, Ti)
G628	0	29.39	18.18	12.68	1.02	15.22	9.61	0	13.90	0
M628	0	27.84	15.63	12.14	1.09	14.30	11.72	0	17.28	0
P628	0	26.12	15.86	15.24	1.49	0	16.80	0	24.49	0
G629	0	21.44	10.02	10.50	1.96	10.72	17.55	0.88	26.94	0
M629	0	23.83	11.83	12.51	1.25	13.30	14.40	0	22.88	0
P629	0	25.74	13.20	11.83	1.31	11.46	14.08	0.73	21.07	0.58
G630	0	25.99	13.59	13.51	0.90	14.42	11.92	0.97	18.36	0.34
M630	0	15.67	8.26	7.36	2.86	6.08	21.60	1.47	36.25	0.45
P630	0	20.18	7.51	11.00	2.45	9.70	18.59	1.43	29.13	0
G631	0	13.34	4.88	5.65	2.71	4.46	23.77	2.40	42.79	0
M631	0	11.84	3.56	5.45	3.18	3.89	24.85	2.64	44.59	0
P631	0	9.14	2.72	4.60	3.38	2.80	27.48	2.93	46.96	0
G632	0	14.19	4.68	6.88	2.74	5.24	22.35	3.21	40.71	0
M632	0	10.24	3.04	5.38	3.19	3.42	25.19	3.35	46.18	0
P632	0	12.96	5.06	7.61	2.13	5.87	23.02	3.14	40.21	0
G633	0	8.89	2.91	3.99	3.33	2.20	24.97	5.12	48.59	0
M633	0	8.25	2.38	3.98	2.95	1.79	25.77	4.98	49.90	0
P633	0	6.92	2.03	3.64	3.40	1.67	26.32	5.38	50.64	0
G634	0	9.63	2.52	5.48	2.92	3.27	22.93	6.82	46.42	0
M634	0	12.75	5.23	8.14	2.07	5.90	19.91	6.08	39.92	0
P634	0	9.77	2.60	4.74	3.65	2.43	22.83	6.68	47.30	0
G635	0	9.94	2.12	4.39	3.30	2.00	21.41	8.37	48.48	0
M635	0	8.04	1.96	3.48	3.27	1.18	22.86	8.60	50.62	0
P635	0	10.16	2.15	4.30	3.19	2.07	21.73	8.49	47.91	0

***G = large sphere; M = medium sphere; P = small sphere**

Then the cast spheres have been pickled with hydrofluoric acid and rinsed in an ultrasonic washing tank, and pictures of the surface have again been taken with the stereoscopic microscope (magnification 10x), Figure 6.

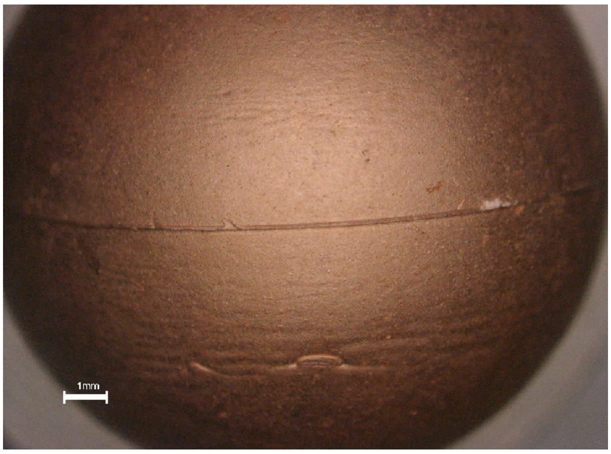

Sample 628

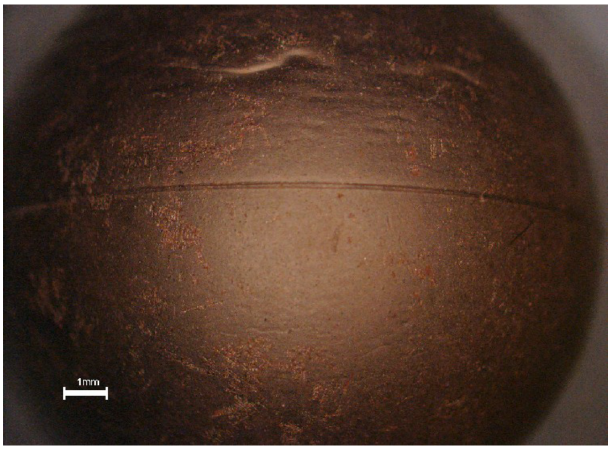

Sample 629

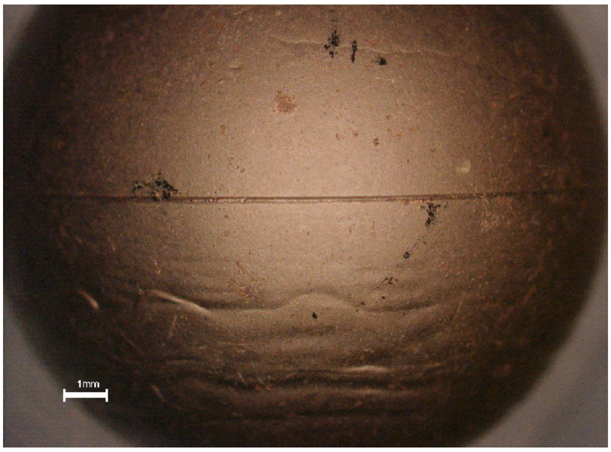

Sample 630

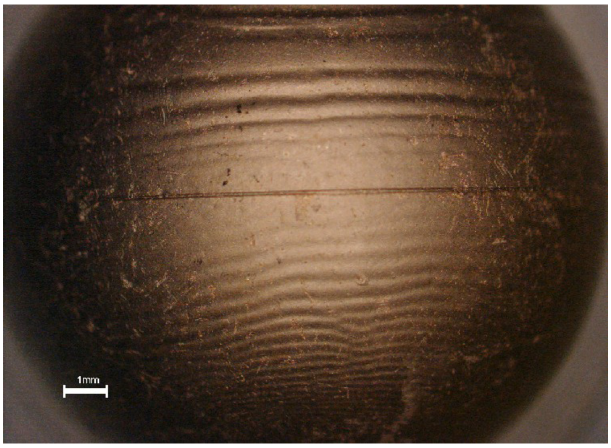

Sample 631

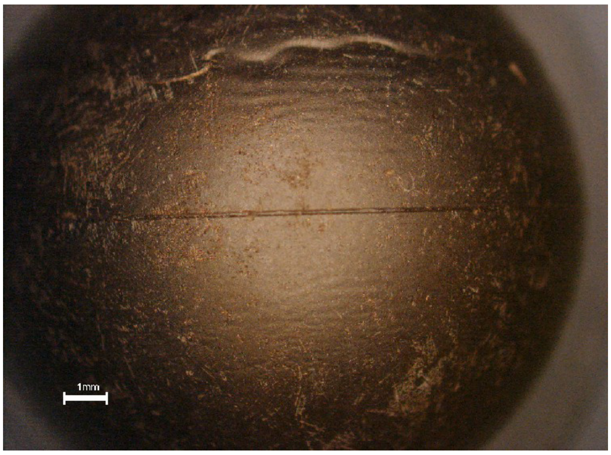

Sample 632

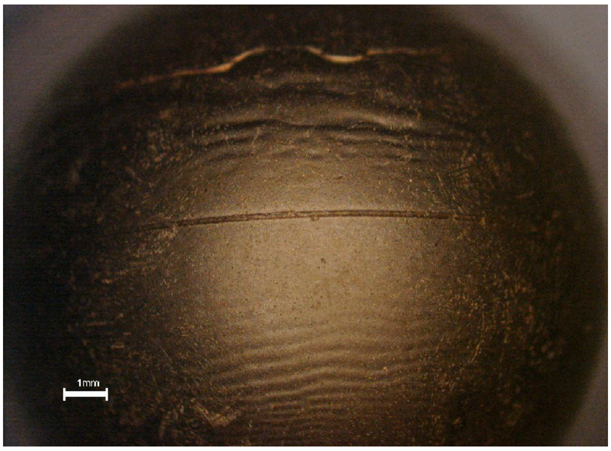

Sample 633

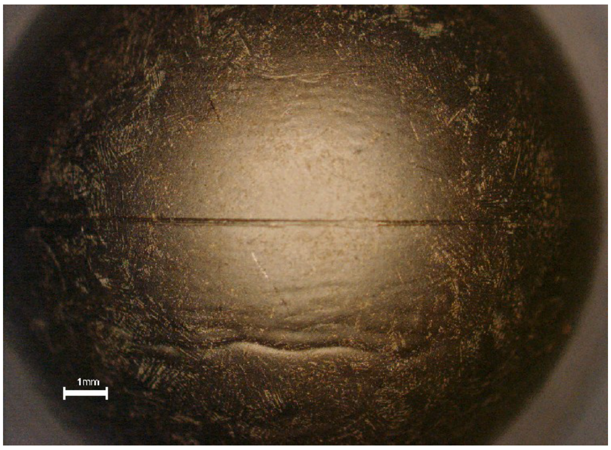

Sample 634

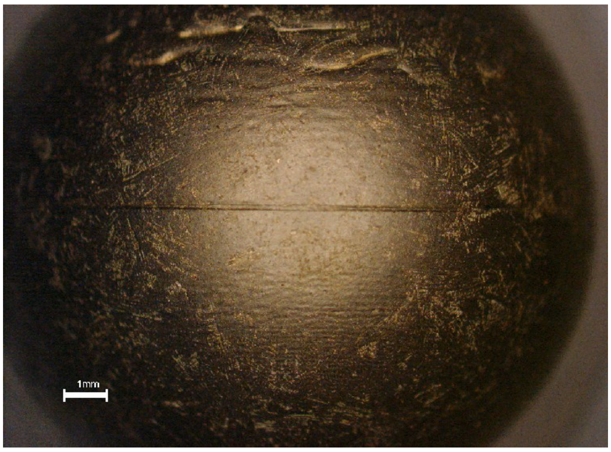

Sample 635

Figure 6 – Surface of the Si containing castings after pickling with hydrofluoric acid (Samples 628 to 635)

Also in this case the samples have again been submitted to SEM microanalysis in the same places as before. The results are shown in Table 5.

Table 5 – Silicon containing castings (Samples 628 to 635). Surface composition after pickling with hydrofluoric acid

sample	Elements [wt%]									
	C	O	Si	S	Ag	Ca	Cu	Zn	Au	Others(Mg, K, Al, Ti)
G628	0	5.58	3.59	0	4.92	0	32.10	0	53.81	0
M628	0	3.72	2.43	0	4.63	0	33.23	0	56.00	0
P628	0	6.01	3.72	0	4.49	0	31.65	0	54.12	0
G629	0	2.58	1.57	0	5.35	0	32.81	1.31	56.38	0
M629	0	2.08	1.38	0	5.35	0	33.47	1.12	56.6	0
P629	0	2.30	1.69	0	4.84	0	33.16	1.24	56.77	0
G630	0	2.50	1.95	0	4.82	0	31.88	2.26	56.13	0
M630	0	2.96	1.61	0	4.06	0	32.83	2.15	56.39	0
P630	0	1.55	1.70	0	3.97	0	33.07	2.38	57.96	0
G631	0	2.15	1.23	0	4.53	0	31.98	3.18	56.93	0
M631	0	1.66	1.04	0	5.65	0	31.63	3.26	56.76	0
P631	0	1.90	1.30	0	5.21	0	30.73	3.32	57.55	0
G632	0	1.78	1.09	0	5.84	0	30.22	4.05	57.03	0
M632	0	1.52	0.97	0	4.62	0	30.52	4.33	58.06	0
P632	0	1.39	0.98	0	5.42	0	30.59	4.11	57.50	0
G633	0	1.53	0.87	0	4.65	0	29.29	6.14	57.51	0
M633	0	1.57	0	0	4.68	0	29.40	6.28	58.07	0
P633	0	1.19	0.57	0	4.41	0	29.43	6.12	58.28	0
G634	0	0.96	0	0	4.51	0	27.63	8.18	58.72	0
M634	0	1.50	0	0	4.68	0	28.14	8.16	57.53	0
P634	0	1.37	0	0	5.35	0	27.41	7.78	58.09	0
G635	0	0.95	0	0	4.84	0	26.27	9.90	58.04	0
M635	0	1.06	0	0	4.60	0	26.19	10.05	58.11	0
P635	0	0.96	0	0	4.47	0	26.32	9.98	58.27	0

***G = large sphere; M = medium sphere; P = small sphere**

After this set of analyses, all samples have been cut along a great circle parallel to the axis of the feed sprue.

SEM microanalyses have been carried out on the cut surface of the samples, to look for possible composition gradients inside the spheres. Namely, the analyses have been carried out at increasing distance from the outer surface of the spheres, i.e. at 0 – 2 – 4 – 6 – 8 –10 –15 – 20 – 25 – 30 µm from the rim of the cut surface. The results are shown in the following chapter.

5. Discussion of the data

The results of the thermal analyses carried out with the Seiko TG/DTA 6300 equipment (TG = thermogravimetric) are shown in Table 6. These data have also been used for selecting the casting temperature of the alloys.

Table 6 – Results of the TG/DTA analyses

Sample	T solidus [°C]	T liquidus [°C]	W1*[mg]	W2* [mg]	100ΔW/ W1
543	895	927	25.97	25.88	0.347
544	890	920	25.63	25.42	0.819
545	882	915	25.69	25.26	1.67
546	875	910	25.34	24.67	2.64
547	865	904	24.82	23.99	3.34
548	850	891	25.1	23.91	4.74
549	837	880	25.21	23.79	5.63
550	817	865	24.47	22.66	7.4
628	896	928	25.66	25.65	0.039
629	883	920	24.07	24.05	0.083
630	871	913	24.86	24.84	0.08
631	863	905	24.57	24.55	0.081
632	859	901	25.33	25.31	0.079
633	841	888	24.99	24.96	0.12
634	822	872	25.07	25.06	0.04
635	810	859	24.88	24.84	0.016

***W1 and W2 = weight of the samples measured during the heating and cooling cycles respectively**

The mass of the samples (W1 and W2) has been recorded during the heating and cooling ramps at a temperature 200°C lower than the maximum temperature of the cycle. In this way all samples have been kept for the same time near the melting temperature, in order to obtain comparable results. Indeed the longer is the time the gold alloy is kept in the liquid state, the more evaporation will take place. Moreover it has been shown that zinc can continue to evaporate even after the solidification of the alloy, so it has been decided to take into account the weights measured at a lower temperature than the solidus temperature.The data on the thermal cycle used for each alloy are shown in Table 7.

Table 7 – Thermal cycles used for each alloy

Sample	T W1-2**[°C]	Heating rate [°C/min]	T max [°C]	Hold time* [minutes]
543	820	10	1020	4
544	815	10	1015	4
545	810	10	1010	4
546	800	10	1000	4
547	800	10	1000	4
548	790	10	990	4
549	770	10	970	4
550	770	10	970	4
628	820	10	1020	4
629	810	10	1010	4
630	810	10	1010	4
631	800	10	1000	4
632	795	10	995	4
633	770	10	970	4
634	770	10	970	4
635	760	10	960	4

***Holding time at the maximum temperature to limit thermic inertia phenomena in the subsequent cooling process.**
****Temperature of the acquisition of the weight of the samples.**

Solidus and liquidus temperatures of the various samples are plotted in Figure 7.

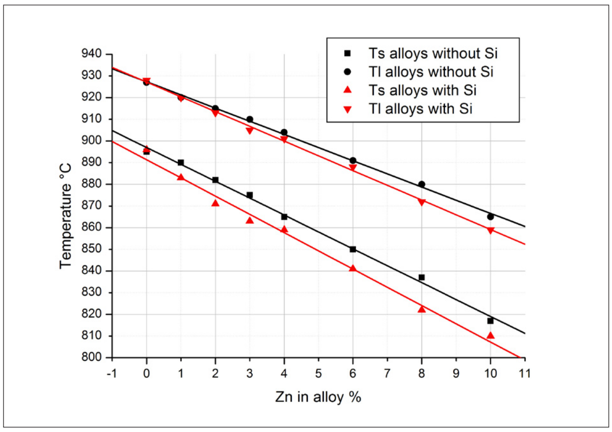

Figure 7 – Solidus and liquidus temperatures of the gold alloys vs. zinc concentration. Ts = solidus temperature; Tl = liquidus temperature

Figure 7 shows that an increase of Zn concentration causes a widening of the melting range. Moreover it can be seen that silicon lowers the solidus temperature more than liquidus temperature. Therefore, for the same zinc content, the melting range of silicon containing alloys is wider than for silicon free alloys. This result confirms the observations already done in practical applications. That is, Si in the alloy “keeps the metal liquid for longer time”.
The percent weight loss has been listed in Table 6 for the different alloys. These data are plotted versus Zn content in Figure 8.

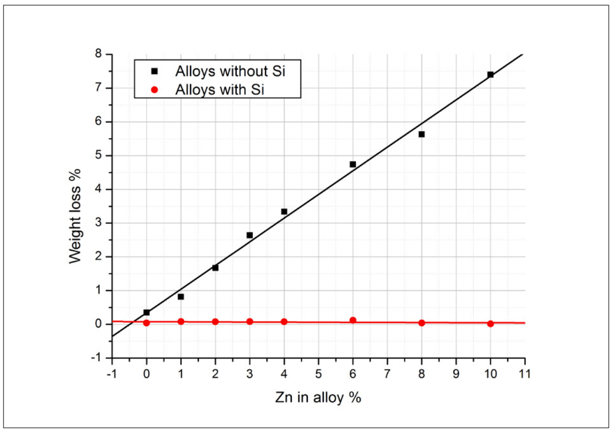

Figure 8 – Percent weight loss of gold alloys versus Zn content

It is evident that weight loss increases proportionally with Zn content in Si-free alloys. This is because Zn is the more volatile component in the gold alloys (the boiling point of Zn is 907°C at the pressure of 1 bar). Therefore it tends to escape more easily from the melt.
The same phenomenon does not occur in Si containing alloys, even with the same Zn content of the Si free alloys. It appears that Si forms a barrier preventing Zn evaporation. Obviously all samples used for the DTA test had been flattened in a press to obtain the same shape and the same exchange area. The appearance of the samples after the DTA test is shown in Figure 9.

Figure 9 – Appearance of the samples after the DTA test.

At first sight, in contrast to the results of other studies, it could appear that in silicon containing alloys there is a lower wettability with higher Zn content, because the samples are gradually less flat (i.e. the contact angle increases). This is the result of a simple visual observation. No specific experiments have been done for evaluating wettability or surface tension. The phenomenon will be investigated in a future study.

Figures 10, 11 and 12 have been obtained from the data listed in Tables 2 and 4, which refer to the as cast samples, after cleaning with a water jet. The surface concentration of different elements is plotted vs. the zinc concentration in the alloys and the samples with added silicon and silicon free samples are compared. In these figures the results from the 3 spheres (large, medium and small) are plotted.

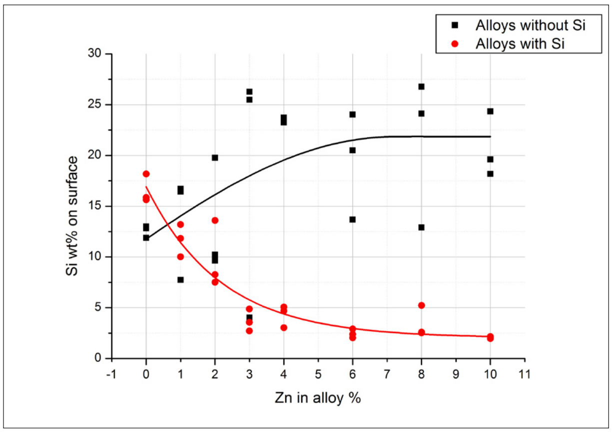

Figure 10 – Si (wt%) on the surface vs. Zn concentration – As cast samples

Relatively high silicon concentration has been found on the surface of silicon free samples, Figure 10. It is presumed that this silicon comes from the silica of the investment. The trend of the curves seems to indicate that silicon free alloys show high reactivity at the interface metal/investment, and reactivity increases with increasing Zn concentration.

As for the silicon containing alloy, we can see that Si concentration on the surface is similar to Si free alloys for low Zn concentration, but decreases with increasing Zn content. Therefore the extent of the reaction between metal and investment appears to decrease with increasing Zn content. This effect could be ascribed to an interaction between Zn and Si.

As for sulphur concentration (sulphur comes from the decomposition of calcium sulphate), we see that in Si free alloys sulphur content is nearly constant with increasing Zn concentration, Figure 11, while in Si containing alloys sulphur concentration decreases with increasing Zn concentration.

Also in this case it appears that Zn lowers interface reactivity, when it is associated with Si.

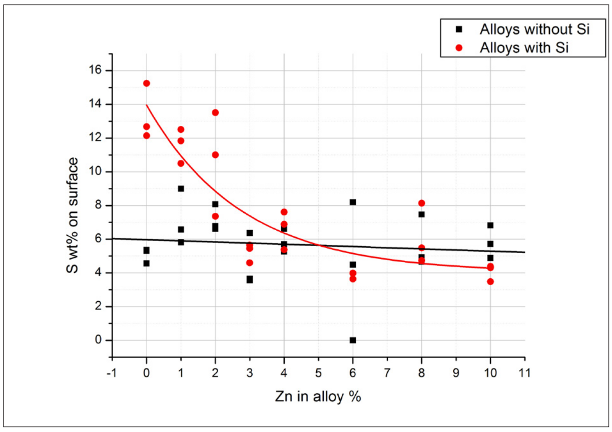

Figure 11 – Plot of sulphur concentration in the surface vs. Zn concentration in the alloy – As cast samples

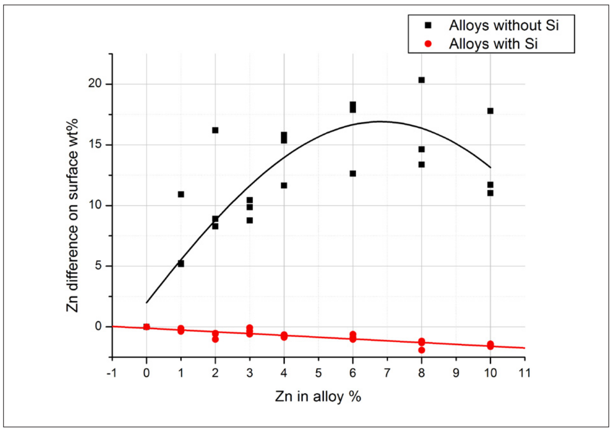

Figure 12 – Plot of the increment of Zn concentration in the surface vs. Zn concentration in the alloy – As cast samples

The increment of Zn concentration on the surface of the castings vs. the zinc concentration in the alloy is plotted in Figure 12. Zn concentration in the alloy has been subtracted from Zn concentration in the surface to compensate for the increase of Zn concentration in the experimented alloys.

An increase of Zn concentration in the surface is evident for the Si free alloys. A high Zn concentration is considered as a clue of the metal/investment interaction. This observation could corroborate the previous observations indicating that zinc favours the reaction with the investment.

In the case of the Si containing alloys, Zn concentration in the surface is similar to Zn concentration in the bulk alloy, with a slightly decreasing trend with increasing Zn concentration in the bulk and concentrations are reached that are slightly lower than bulk concentration. Therefore Si containing alloys should show a rather low reactivity with the investment, as already suggested by the visual inspection.

Silver and gold have been considered as an index of reaction intensity at the metal/investment interface. Therefore the absence of noble metals in the surface of the as cast Si free spheres suggests that base metal components of the alloys strongly reacted with the investment, with the formation of the thick surface layer that is observable in the photographs, Figure 2. In the spheres of Si containing alloys, where a lower reactivity is presumed, a higher Ag concentration is observed, Figure 13. Moreover an increased Zn concentration corresponds to a higher Ag content. This trend could confirm the synergic effect of Zn and Si for the protection of the melt during the casting process.

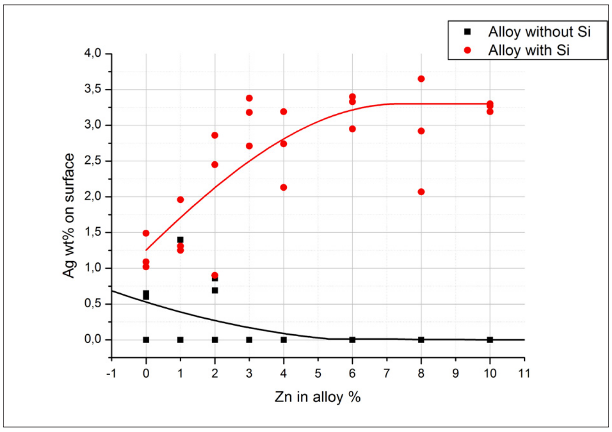

Figure 13 – Silver concentration in the surface vs. Zn bulk concentration – As cast samples

Gold shows a behaviour very similar to silver, Figure 14, and the same considerations made for silver apply also in this case.

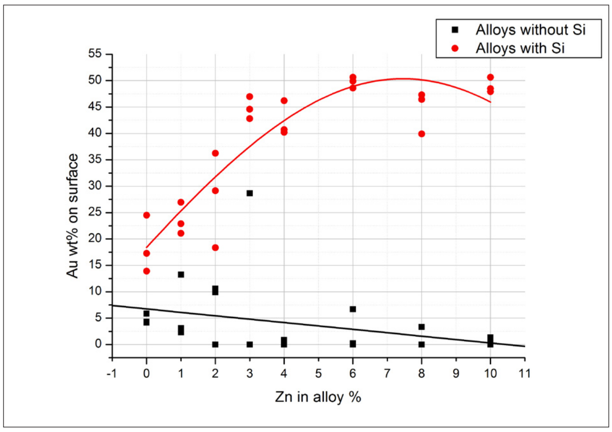

Figure 14 – Au concentration in the surface vs. Zn bulk concentration – As cast samples

A set of plots follows regarding the microanalysis of the surface of the spheres after pickling with hydrofluoric acid.

Silicon free alloys do not show traces of Si in the surface, Figure 15. This result corroborates the hypothesis that the Si observed on the surface of the as cast spheres comes from a reaction with the investment. This reaction could form a layer of reaction products on the surface that is completely removed by the acid.

On the contrary, the spheres of Si containing alloys (samples 628 to 633) show a surface Si concentration much higher than in the bulk. With increasing Zn concentration, Si concentration goes down and in samples 634 and 635 it becomes close to zero.

Such a high Si concentration could indicate a strong reaction between metal and investment. But these high values have been observed after pickling with hydrofluoric acid and we could presume that the silicon to metal bond should be different from the bond formed in the Si free alloys.

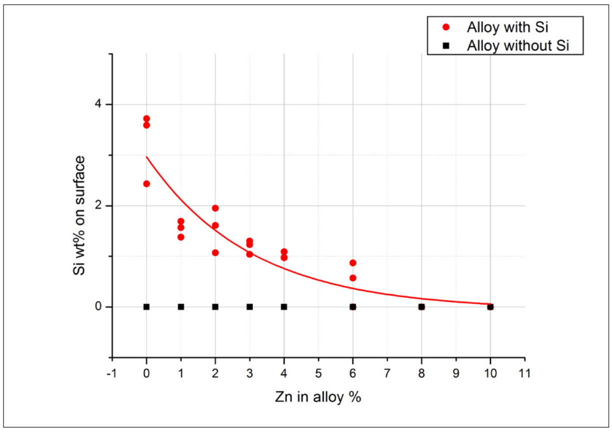

Figure 15 – Si concentration in the surface vs. Zn concentration in the bulk – After pickling

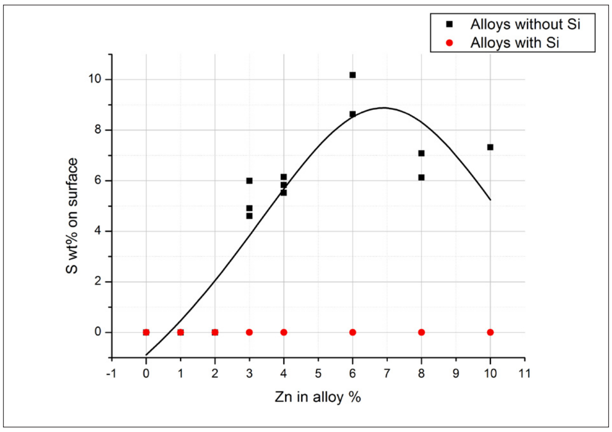

Figure 16 – Sulphur concentration in the surface vs. Zn concentration in the bulk – After pickling

In the Si free alloys (samples 543 to 550) there is an increase of surface sulphur concentration with increasing bulk concentration of Zn, Figure 16. This could also be interpreted as a clue of reactivity, because the sulphur can only come from the decomposition of calcium sulphate with formation of sulphur dioxide which subsequently caused the formation of sulphides in the surface (CuS, ZnS).

The results of sulphur determination confirm that Si containing alloys show a low reactivity with calcium sulphate: no trace of sulphur has been found on the surface after pickling.

As for Zn, also in this case the increment of Zn surface concentration compared to the bulk concentration has been considered, Figure 17.

After removing the surface layer of reaction products with the acid, the Si free samples show a surface concentration of Zn lower than in the bulk alloy. This results suggests that part of the Zn reacted with the investment and has been removed by acid pickling. On the contrary, in the Si containing samples surface Zn concentration is very near to the Zn concentration in the bulk, and the behaviour observed on the spheres before pickling has been confirmed. Thus it is presumed that zinc did not react with the investment. In this case too experimental observation confirms the Si-Zn synergy for protecting the melt from reaction with the investment (higher Zn bulk concentration corresponds to a surface concentration nearer to bulk concentration).

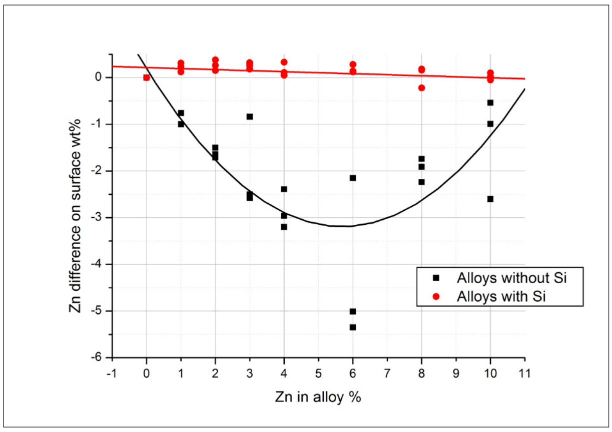

Figure 17 – Plot of the increment of Zn concentration in the surface vs. Zn concentration in the bulk - After pickling

As for silver, after pickling in hydrofluoric acid, in the Si containing samples surface Ag concentration is constant and very near to bulk concentration, Figure 18. This fact denotes a low reactivity of this metal.

In Si free samples the surface concentration of Ag decreases with increasing Zn content in the bulk. This phenomenon could be ascribed to the fact that hydrofluoric acid didn't remove all reaction products (see the trend for sulphur, Figure 16), mainly in the samples with higher Zn content, where a stronger reaction occurred. We could presume that in this last case the products of the metal-investment reaction formed a stronger bond with the metal matrix.

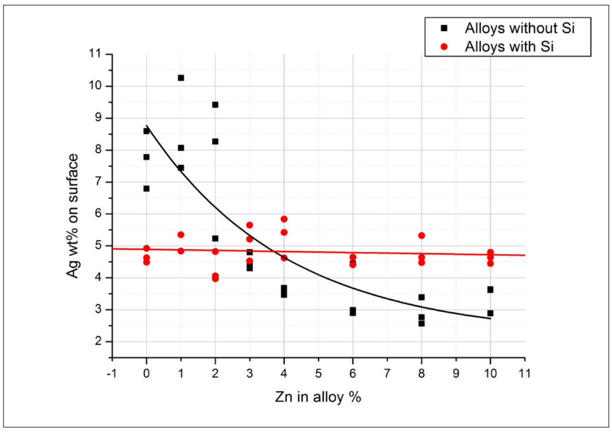

Figure 18 – Plot of Ag concentration in the surface vs. Zn concentration in the bulk – After pickling

Gold behaviour is very similar to silver, Figure 19.

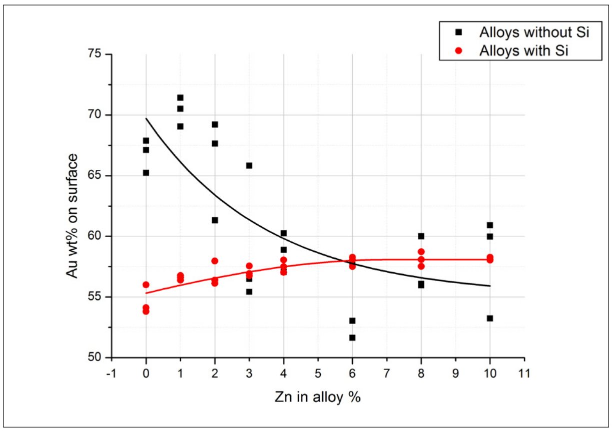

Figure 19 – Plot of Au concentration in the surface vs. Zn concentration in the bulk – After pickling

The above analyses showed that the size of the spheres does not affect the results. Therefore we addressed our research only to the bigger spheres.

After analysing the outer surface, the alloy composition inside the spheres has been investigated. Therefore a mapping of the composition on the cross section of the spheres has been carried out, as previously described. The plots of the obtained results are shown in the following pages.

6. Variation of Zn concentration in the cross section

The results of Zn determination in the cross section of the large spheres are plotted in Figures 20 to 26 (samples 544 to 550 and 629 to 635) .

The Si free samples (544 to 550) show an increasing Zn concentration from the surface of the sphere towards the centre. After about 30 µm, Zn concentration is similar to the bulk concentration.

In Si containing samples (629 to 635) Zn concentration shows a different trend: it is nearly constant and similar to bulk concentration. Actually it is slightly lower than the bulk value, but it can be an instrumental error and anyway we are interested only in a comparison of the trends of the different elements.

Generally, for the same bulk concentration, Si containing alloys show a higher Zn concentration near the surface. The Zn bulk concentration is approximately the same for Si containing and Si free alloys.

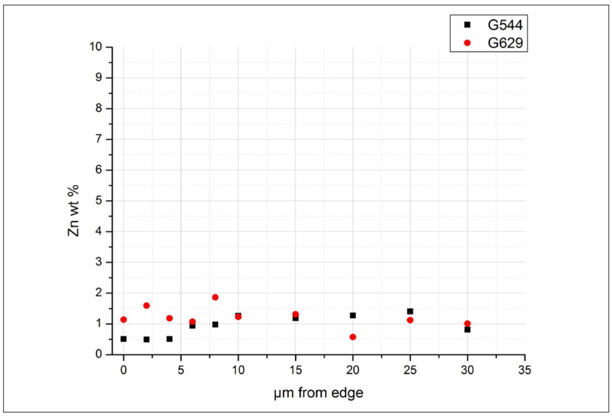

Figure 20 – Plot of zinc concentration in the cross section of the spheres (Samples 544 and 629)

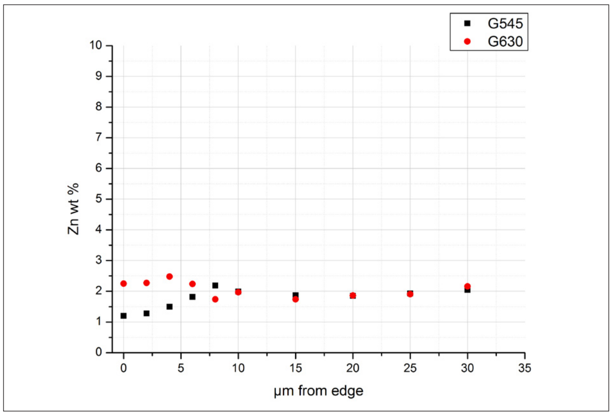

Figure 21 – Plot of zinc concentration in the cross section of the spheres (Samples 545 and 630)

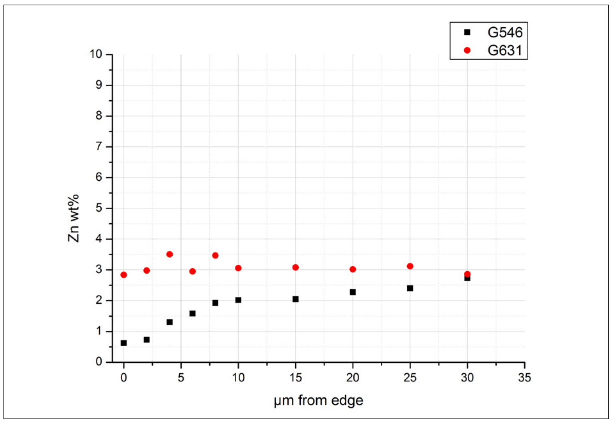

Figure 22 – Plot of zinc concentration in the cross section of the spheres (Samples 546 and 631)

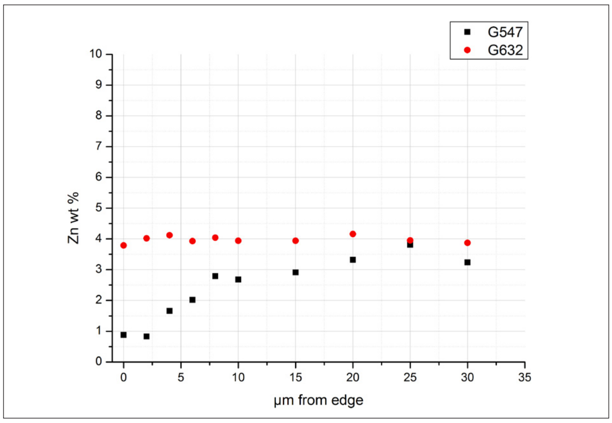

Figure 23 – Plot of zinc concentration in the cross section of the spheres (Samples 547 and 632)

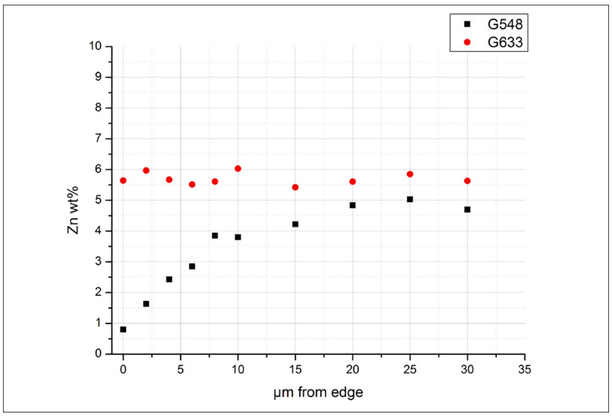

Figure 24 – Plot of zinc concentration in the cross section of the spheres (Samples 548 and 633)

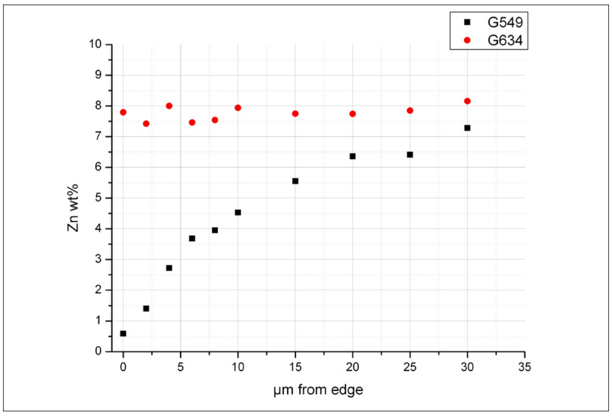

Figure 25 – Plot of zinc concentration in the cross section of the spheres (Samples 549 and 634)

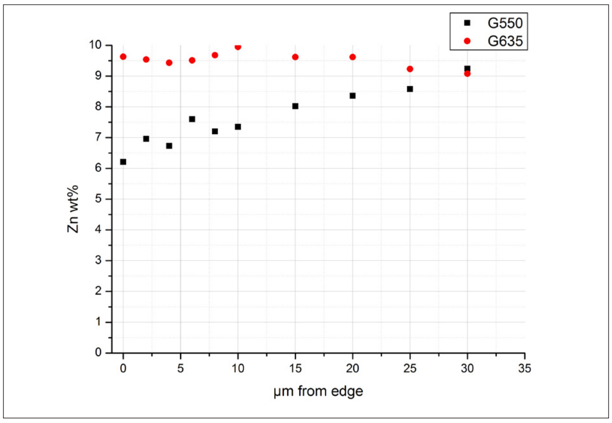

Figure 26 – Plot of zinc concentration in the cross section of the spheres (Samples 550 and 635)

7. Variation of Cu concentration in the cross section

(Figures 27 to 34)

Si free samples (543 to 550) show a slightly lower Cu concentration in the first few µm near the surface. Deeper in the sample, Cu concentration becomes nearly constant. Generally Si free alloys show higher Cu concentration than the alloys with Si addition. In this case too, after 15 to 20 µm from the surface of the sphere, Cu concentration is similar in Si free and Si containing alloys.

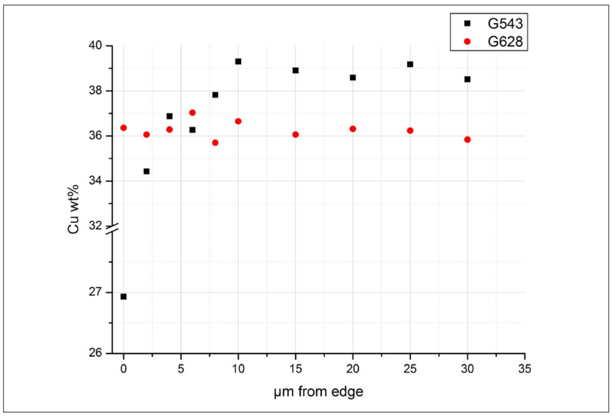

Figure 27 – Plot of Cu concentration in the cross section of the spheres (Samples 543 and 628)

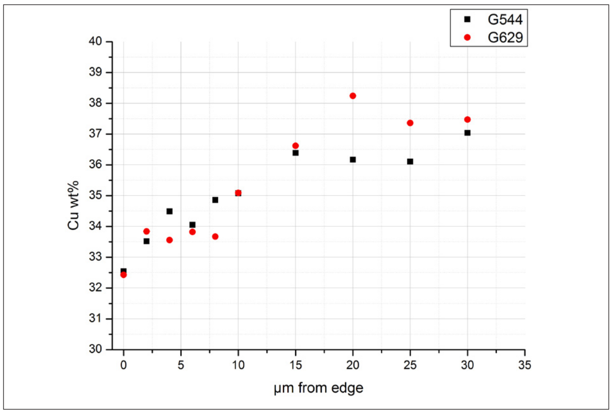

Figure 28 – Plot of Cu concentration in the cross section of the spheres (Samples 544 and 629)

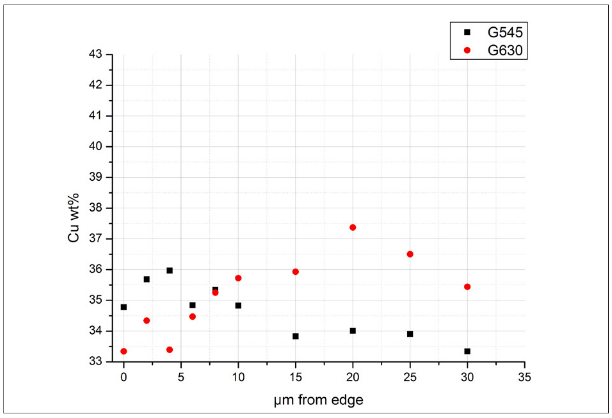

Figure 29 – Plot of Cu concentration in the cross section of the spheres (Samples 545 and 630)

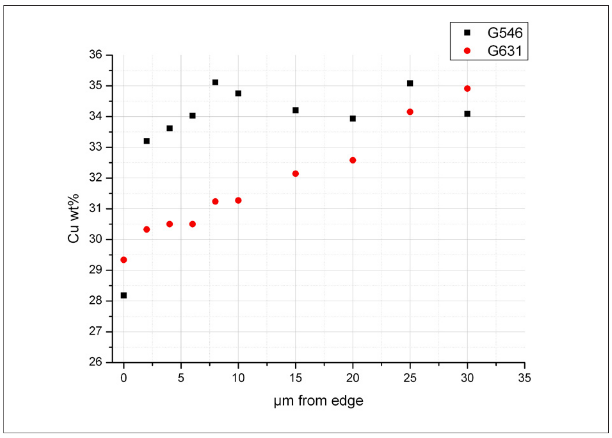

Figure 30 – Plot of Cu concentration in the cross section of the spheres (Samples 546 and 631)

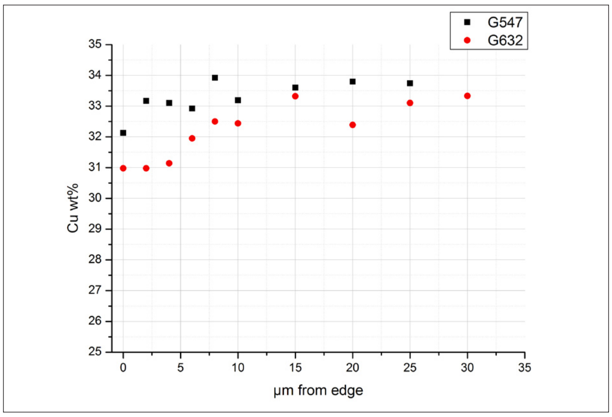

Figure 31 – Plot of Cu concentration in the cross section of the spheres (Samples 547 and 632)

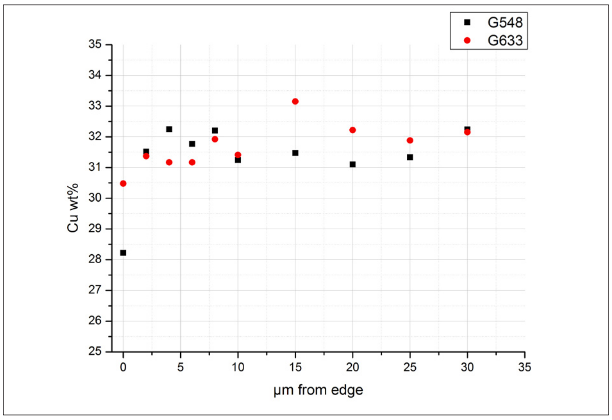

Figure 32 – Plot of Cu concentration in the cross section of the spheres (Samples 548 and 633)

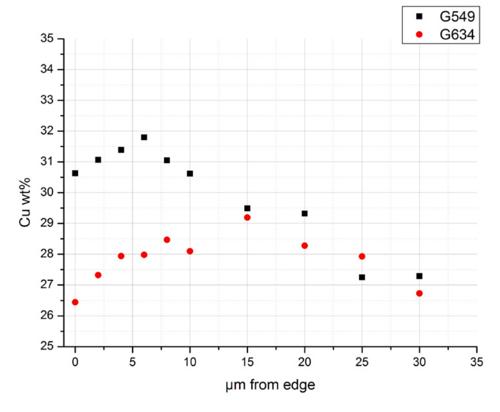

Figure 33 – Plot of Cu concentration in the cross section of the spheres (Samples 549 and 634)

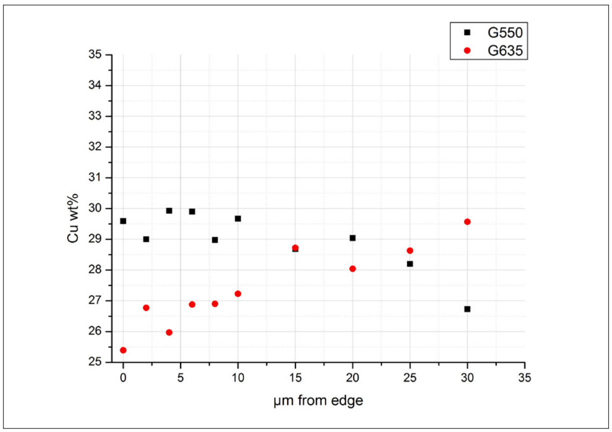

Figure 34 – Plot of Cu concentration in the cross section of the spheres (Samples 550 and 635)

8. Variation of Ag concentration in the cross section

(Figures 35 to 42)

In the Si free samples (543 to 550) the trend of Ag variation is less well defined than for Zn. Samples 543 and 544, Figures 35 and 36, show an Ag concentration decreasing from the surface to the inner part of the sphere, where it becomes similar to bulk concentration. Samples 545 to 550 show a nearly constant Ag concentration, similar to the bulk value.

The behaviour of Ag in the Si containing samples (628 to 635) is similar to Si free samples (543 to 550) with some exception (see sample 631).
In this case too, for the same composition, the alloys with Si addition show higher Ag concentration near the surface, and Ag concentration in the bulk is similar for both Si free and Si containing alloys. In the case of Ag this behaviour is less evident than in the case of Zn.

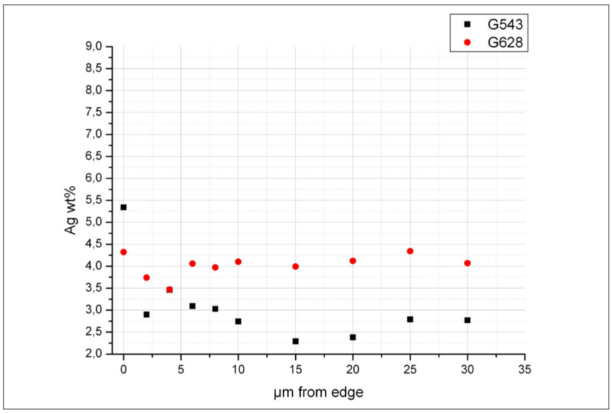

Figure 35 – Plot of Ag concentration in the cross section of the spheres (Samples 543 and 628)

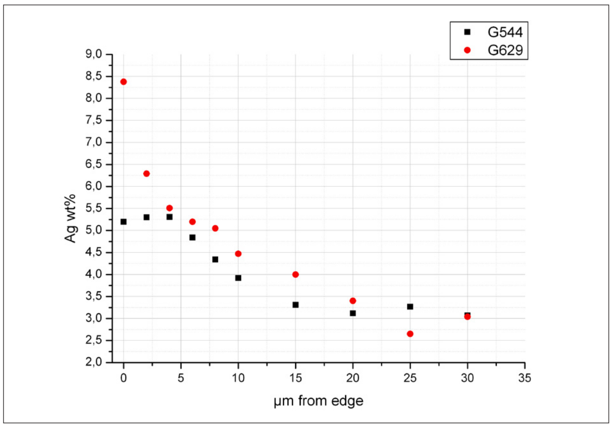

Figure 36 – Plot of Ag concentration in the cross section of the spheres (Samples 544 and 629)

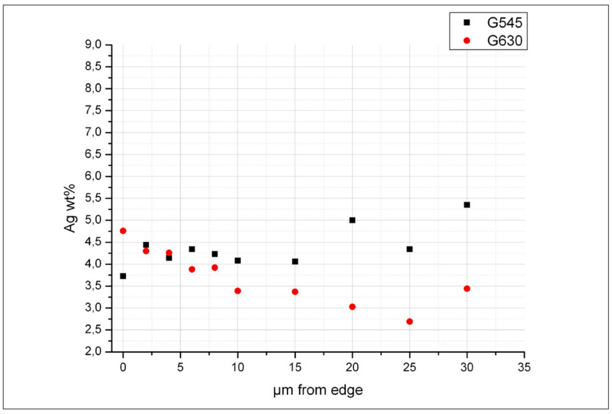

Figure 37 – Plot of Ag concentration in the cross section of the spheres (Samples 545 and 630)

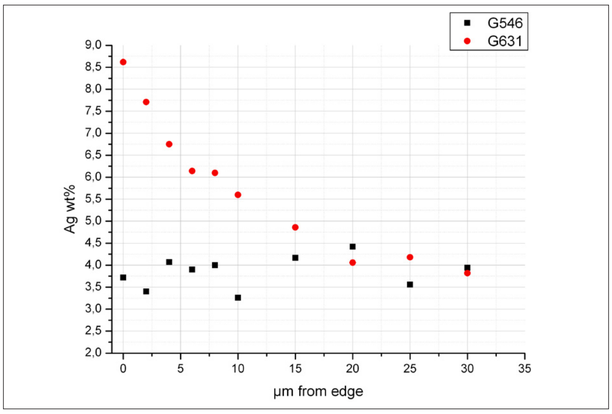

Figure 38 – Plot of Ag concentration in the cross section of the spheres (Samples 546 and 631)

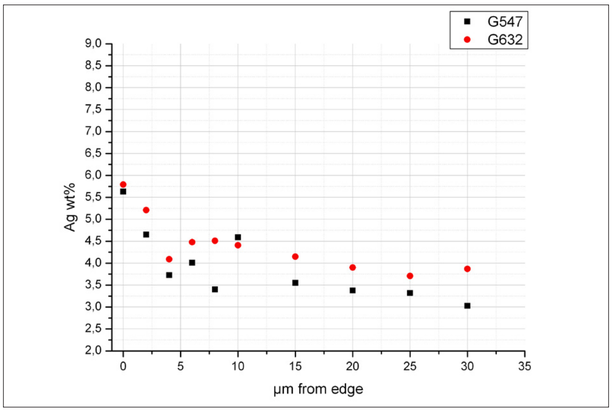

Figure 39 – Plot of Ag concentration in the cross section of the spheres (Samples 547 and 632)

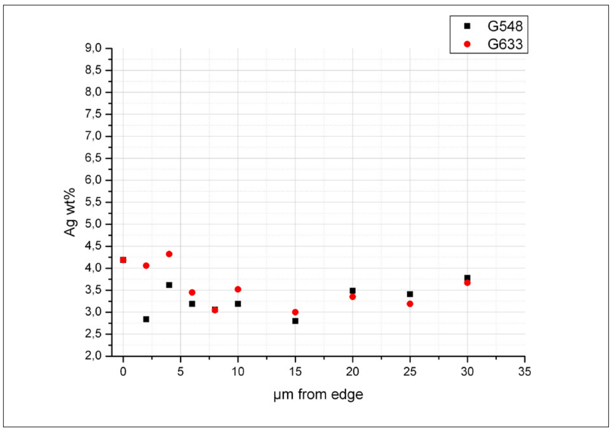

Figure 40 – Plot of Ag concentration in the cross section of the spheres (Samples 548 and 633)

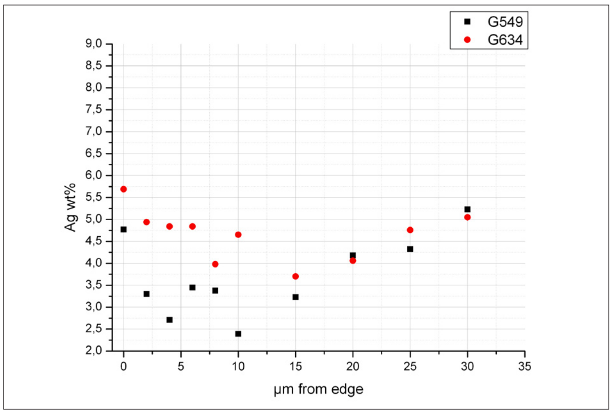

Figure 41 – Plot of Ag concentration in the cross section of the spheres (Samples 549 and 634)

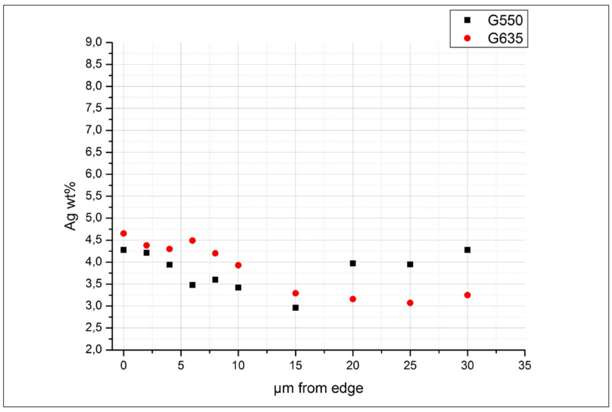

Figure 42 – Plot of Ag concentration in the cross section of the spheres (Samples 550 and 635)

8. Variation of Au concentration in the cross section

Si free samples (543 to 550) show a decreasing Au concentration from the surface to the bulk and surface concentration is appreciably higher than bulk concentration. Si containing samples (628 to 635) show a more constant Au concentration, near to nominal fineness. Generally in Si free samples surface Au concentration is higher than in the Si containing samples. In this case too the difference observed for bulk concentration is minimal.

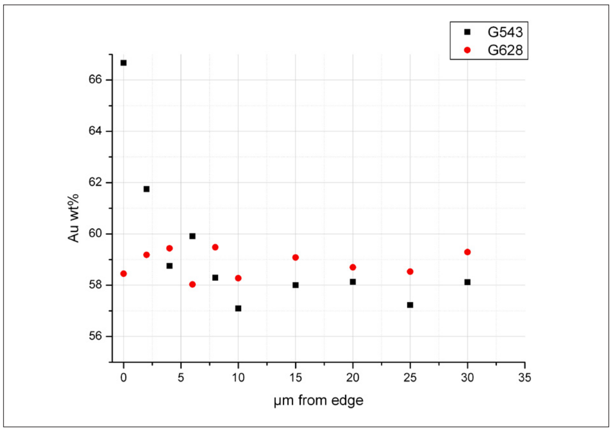

Figure 43 – Plot of Au concentration in the cross section of the spheres (Samples 543 and 628)

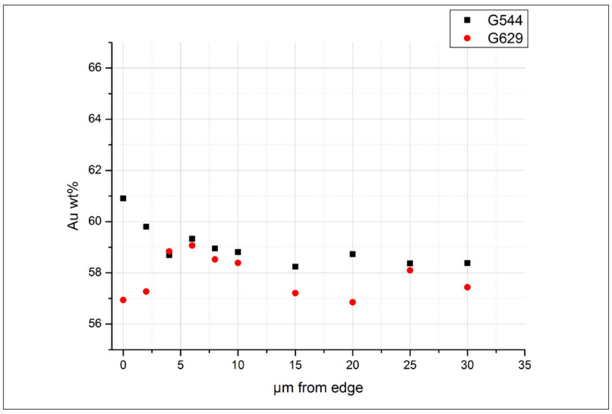

Figure 44 – Plot of Au concentration in the cross section of the spheres (Samples 544 and 629)

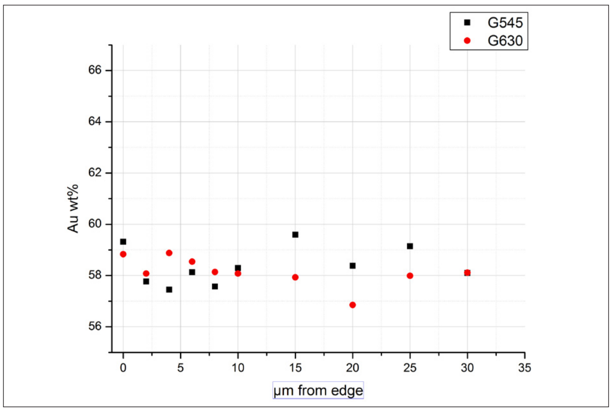

Figure 45 – Plot of Au concentration in the cross section of the spheres (Samples 545 and 630)

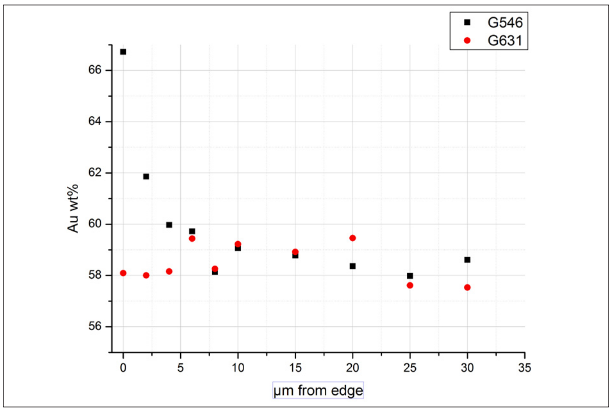

Figure 46 – Plot of Au concentration in the cross section of the spheres (Samples 546 and 631)

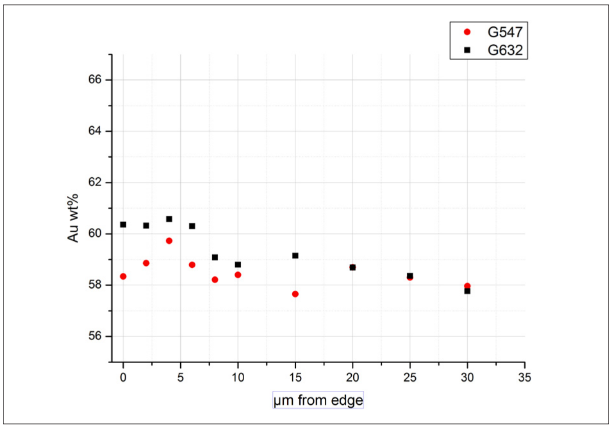

Figure 47 – Plot of Au concentration in the cross section of the spheres (Samples 547 and 632)

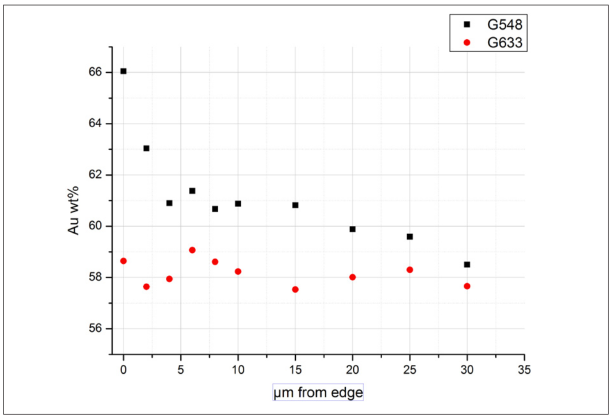

Figure 48 – Plot of Au concentration in the cross section of the spheres (Samples 548 and 633)

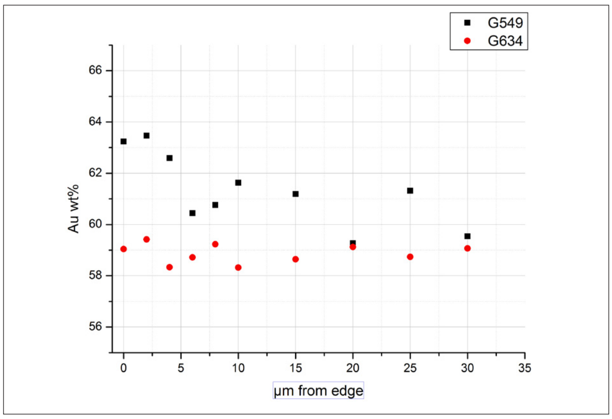

Figure 49 – Plot of Au concentration in the cross section of the spheres (Samples 549 and 634)

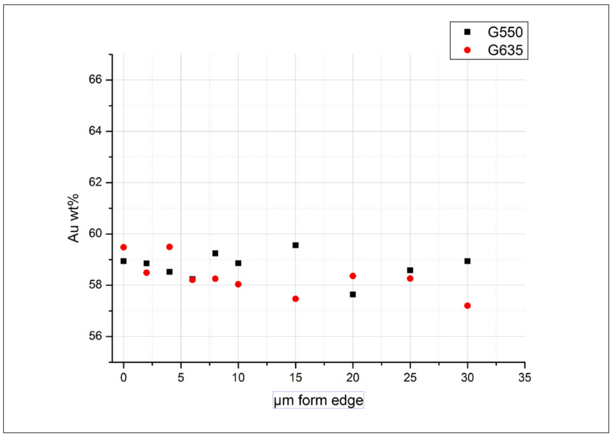

Figure 50 – Plot of Au concentration in the cross section of the spheres (Samples 550 and 635)

The cross section of the spheres has also been inspected for defects (particularly near the surface of the sphere), looking for any correlation that could be present between defects and a reaction with the investment. No correlation has been found between alloy composition and porosity. Porosity appears randomly distributed with an aspect similar to shrinkage porosity. No evident gas porosity has been observed.

After the inspection for defects, the microstructure of the 16 alloys has been observed on the cross section of the spheres, Figure 51.

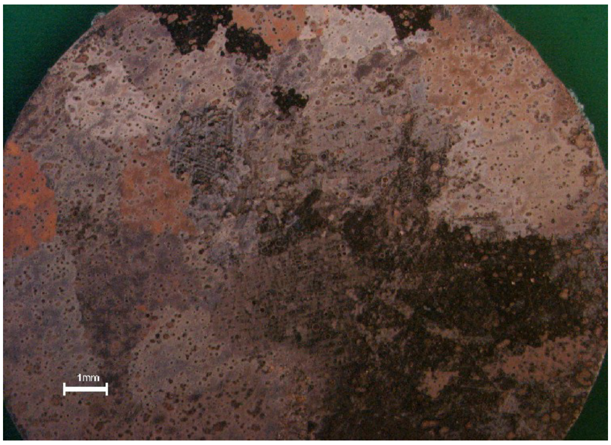

Sample 543

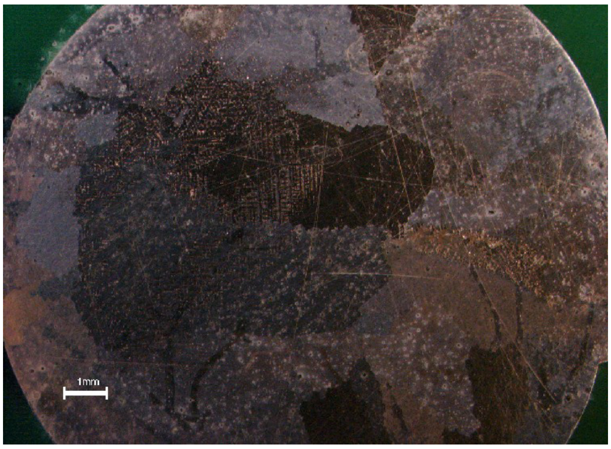

Sample 628

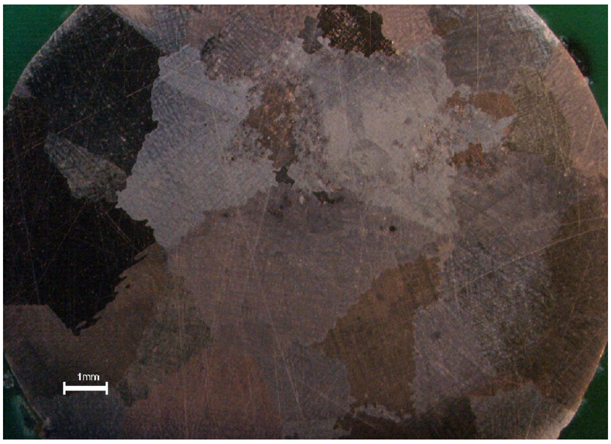

Sample 544

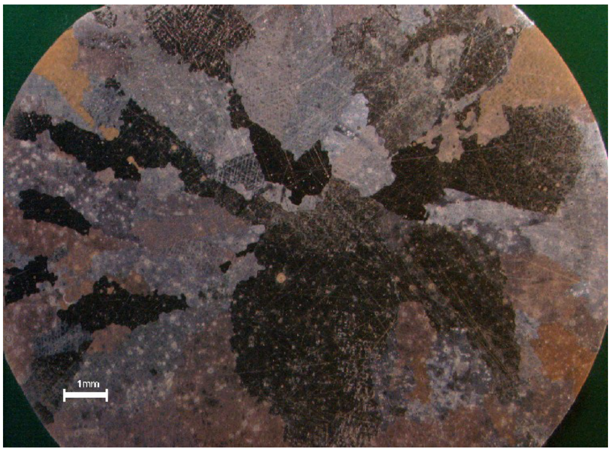

Sample 629

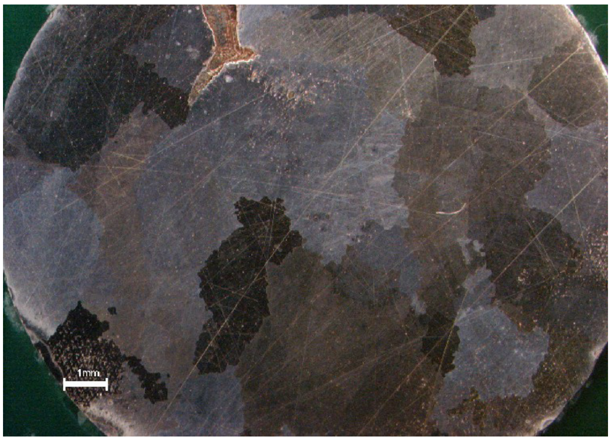

Sample 545

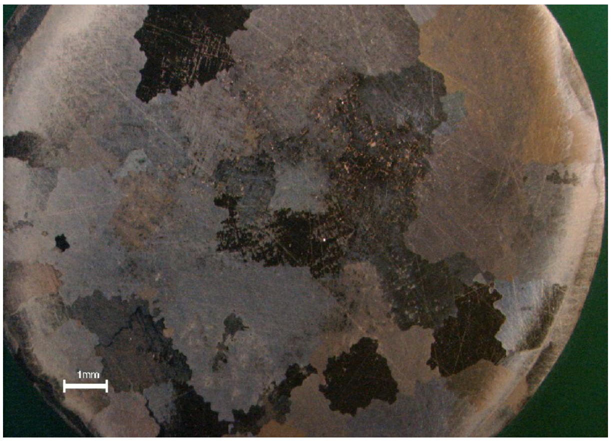

Sample 547

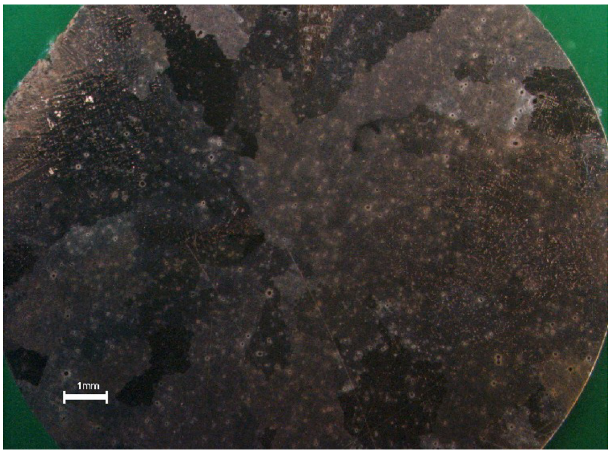

Sample 630

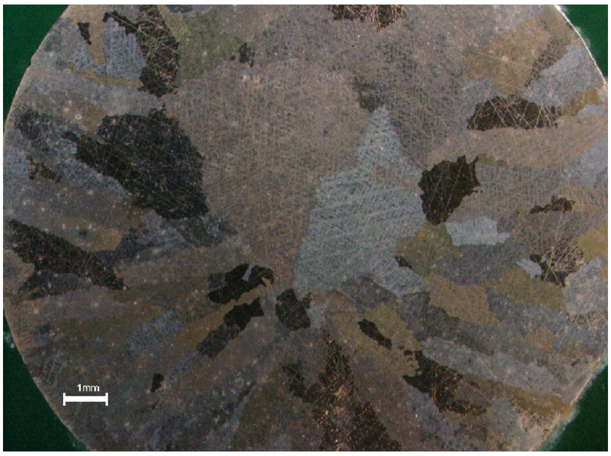

Sample 632

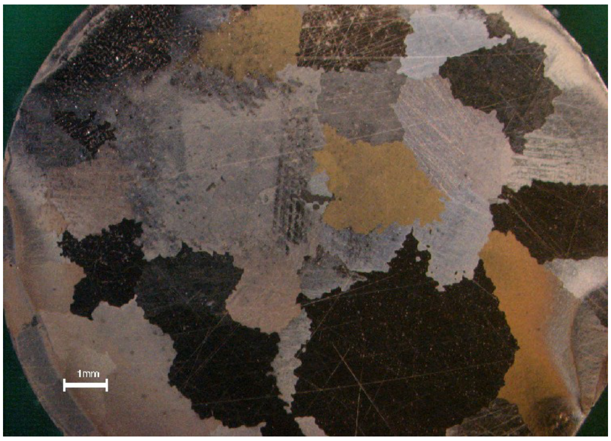

Sample 546

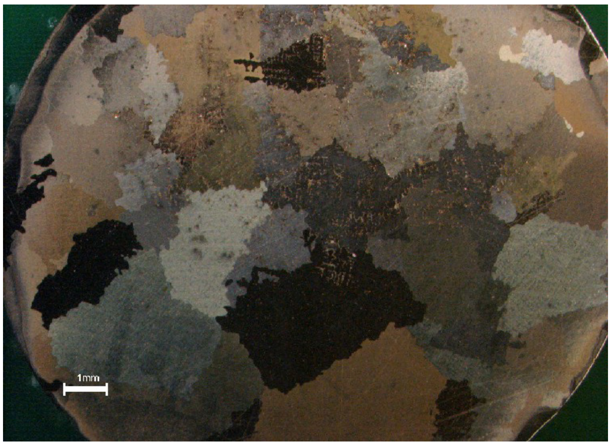

Sample 548

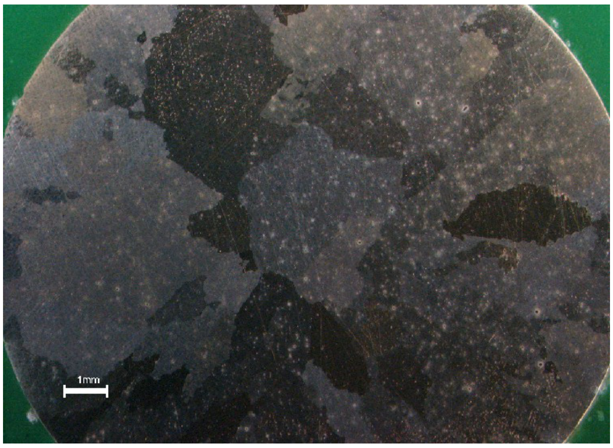

Sample 631

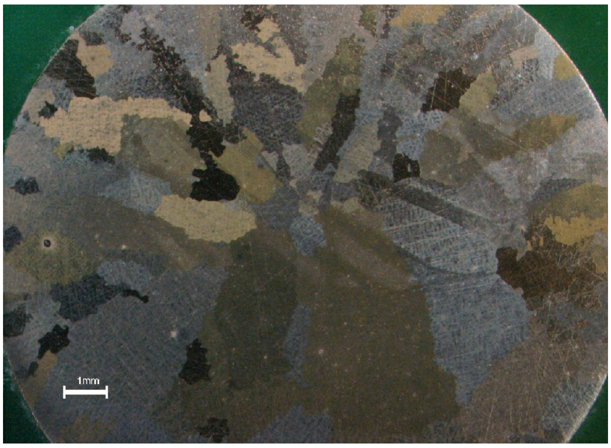

Sample 633

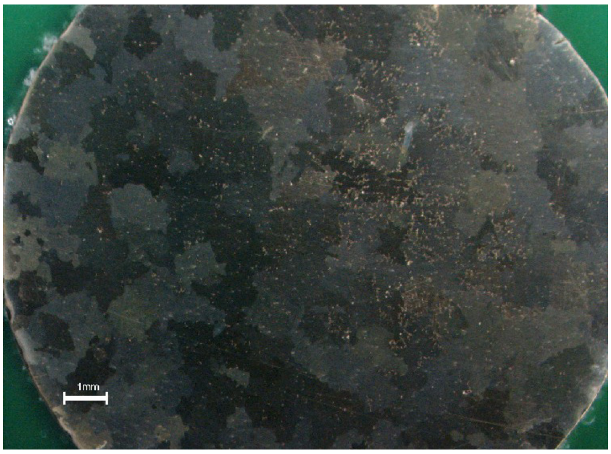

Sample 549

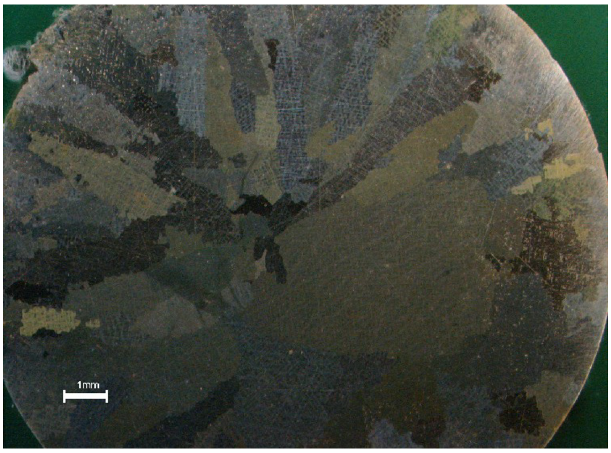

Sample 634

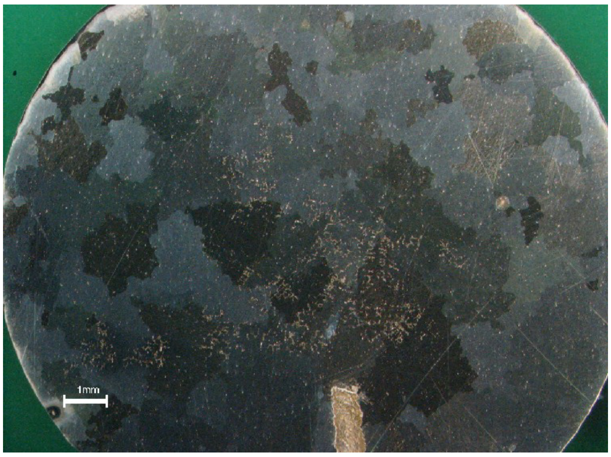

Sample 550

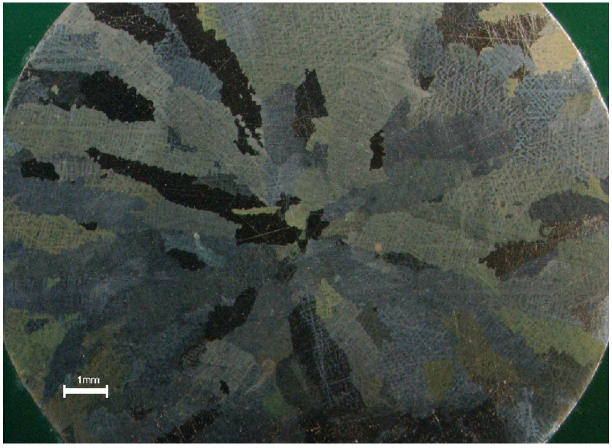

Sample 635

Figure 51 – Micrographs of the cross section of the spheres

The difference of crystal grain structure between Si free alloys and Si containing alloys is evident. Si free alloys show an equiaxed grain structure, while the Si containing alloys show a columnar grain.

The crystal growth mechanism during solidification is strongly affected by the temperature gradient in the melt, but is also affected by the presence of additions. Some elements or compounds cause the formation of a large number of solidification nuclei and are known as “grain refiners”. Si, on the contrary, hinders the formation of solidification nuclei, so metal crystals are nucleated mainly on the mould wall and the crystals grow inwards from the wall, in the direction of the temperature gradient, forming a columnar grain structure.

9. Conclusions

Firstly we should remark that there is no significant difference in the composition of the surface layer for spheres of different size. Therefore the mass of the castings had no significant effect on the reaction with the investment.

The analysis of the effects of the different alloying elements is much more complex.

The obtained results and the appearance of the surface of the casting brought us to presume that in Si containing samples the intensity of the reaction with the investment has been substantially lower than in Si free samples.

Moreover the results suggest that an increasing deoxidisation effect is observed with increasing Zn concentration, when Si is present. On the contrary, in Si free alloys an increased Zn concentration corresponds to a stronger oxidation of the surface. This observation is corroborated by the Zn and S concentration measured on the surface, Figures 11, 12, 16 and 17.

The results of the microanalyses did not enable us to describe univocally the nature of the interaction between metal and investment, but nevertheless interesting clues for further investigation have been obtained.

The Si free spheres showed a considerably thick surface layer of reaction products that was ever more deeply connected with the bulk metal with increasing Zn concentration, Figures 15, 16 and 17.

In the Si containing alloys the surface layer of reaction products is much thinner, and grows ever thinner with increasing Zn concentration. This observation is confirmed by the fact that the peak of Au is practically absent in the Si free as

cast samples (samples 543 to 550) and in the Si containing as cast samples (samples 628 to 635) grows stronger with increasing Zn concentration. Since the penetration depth of the X-rays is practically constant in the different samples, the observation of an increasing Au concentration should mean that the surface layer becomes thinner.
This observation can be clarified by Figure 52. In this figure the surface concentration of Cu, Zn and Si and other impurity elements (Au and Ag have been omitted) is plotted vs. Zn bulk concentration.

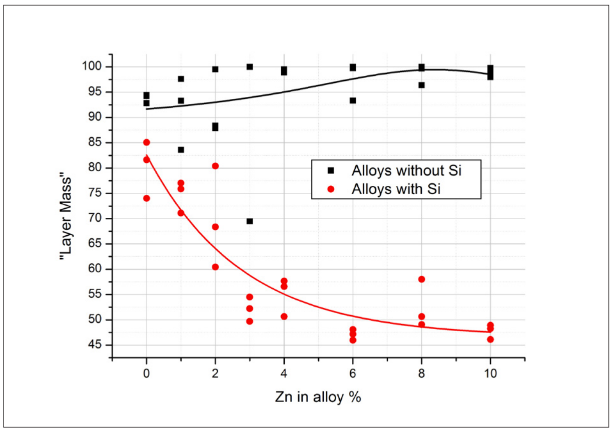

Figure 52 – "Mass" of the surface layer vs. Zn concentration in the alloys

It is clear that in Si containing samples there is a synergic effect between Zn and Si for protecting the surface from oxidation. The components of the surface layer of reaction products could be:

Cu oxides (CuO, Cu2O)
Zn oxide (ZnO)
Cu and/or Zn sulphides (CuS, Cu2S, ZnS)
Zn and/or Cu silicates.

Our results show that zinc silicate could play an important role in this phenomenon.
The DTA tests showed that the presence of Si reduces the weight loss of the melt considerably (The weight loss is ascribed to Zn evaporation). It is believed that Zn evaporation could be prevented by a surface layer covering the melt, that is impermeable to Zn.
The photographs of the Si containing samples (628 to 635), Figure 9, show that the shape of the samples after the TG/DTA test becomes gradually more spherical with an increasing Zn content. It means that the contact angle changes, showing a decrease of wettability with an increasing Zn concentration. This observation corroborates the hypothesis of an interaction between Si and Zn. In fact no change of the contact angle has been observed in the Si free samples.
In our opinion, the results of our work show that the protection of the castings against oxidation should not be ascribed to silicon only, but to the simultaneous effect of Si and Zn. Si and Zn could react simultaneously with oxygen with the formation of a silicate, that becomes interposed between the metal and the investment on the outer surface of the spheres. This layer should prevent the reaction between the melt and the investment and form a barrier against the evaporation of the metallic zinc from the gold alloy.
This hypothesis has been only indirectly substantiated, because it has not been possible to demonstrate the presence of such silicate experimentally. To get more reliable information, further investigation of surface composition is under way and also infrared spectroscopy observations will be performed, to measure bond energy and to look for structures that could confirm the presence of a zinc silicate.
Up to now this work has not been concluded, because also other parameters are presently under study, as the minimum Si concentration required to obtain the desired benefits. This investigation should also help to understand what happens when scrap of Si containing alloys is reused. It should be interesting to evaluate the amount of Si lost in each melting operation, to see if it is affected by Zn concentration in the alloy.
Another parameter requiring further investigation is the effect of a grain refiner on the combined behaviour of Zn and Si.

10. Bibliography

-"Gold alloys", Leach Gal-Or, Proceedings of The Santa Fe Symposium on Jewelry Manufacturing Technology, 1987.

-"Testing the Quality of Jewelry Castings", C.J. Raub, Proceedings of The Santa Fe Symposium on Jewelry Manufacturing Technology, 1987.

-"The Effect of Common Additives on the Cast Properties of 14 Karat Alloys", R. Carrano and J. Derohner, Proceedings of The Santa Fe Symposium on Jewelry Manufacturing Technology, 1988

-"Investment Casting of Gold Jewlry-Factors Affecting the Filling of Moulds", C. Raub and D. Ott, Gold Bulletin, April 1986.

-"Gold Casting Alloys", C. J. Raub and D. Ott, Gold Bulletin, 1983.

-"Compositional Variations Effects on Grain Refeiner Performace in Investment Casting of 14 K Yellow Gold", T. Santala, Proceedings of The Santa Fe Symposium on Jewelry Manufacturing Technology, 1991.

-"The Optimisation of Silicon Alloying Additions in Carat Gold Casting Alloys", G.Normandeau, Gold Technology, April 1995

-"The Evolution of an Alloy", A. Eccles, Proceedings of The Santa Fe Symposium on Jewelry Manufacturing Technology, 1998.

-"The Effect of Various Additives on the Performance of an 18 Karat Yellow Gold Investment Casting Alloy", G. Normandeau, Proceedings of The Santa Fe Symposium on Jewelry Manufacturing Technology, 1996

-"The Effect of Quench Temperature on Silicon Containing Low Carat Investment Casting Alloys", S. Grice, Proceedings of The Santa Fe Symposium on Jewelry Manufacturing Technology, 1999

-"Silicon Microsegregation in 14 K Yellow Gold Jewlery Alloys", J. C. McCloskey, S. Aithal and P.Welch, Gold Bulletin, 2001

-"The Effect of Silicon Deoxidation and Grain Refinement on the Production Performance of a 14 Karat Yellow Gold Casting Alloy", J. C. McCloskey, S. Aithal and P.Welch, Gold Technology 2000.

-"Controlling Melt Loss when Melting Gold Alloys", E.Bell, Jewelry Technology Forum, 2004.

-"Thermochemical and Microstructural Study of Modified Ca2SO4 Bonded Investment with Inorganic and Organic Additives", G.M. Ingo, G. Montesperelli, C. Ricucci, V. Faccenda, A. Bianco, P. Sbornucchia, Proceedings of The Santa Fe Symposium on Jewelry Manufacturing Technology, 2001
-"A Comparision of Burnout Cycle Using an Electric Furnace", I. Mckeer, Proceedings of The Santa Fe Symposium on Jewelry Manufacturing Technology, 2001